REVIEW

Check for updates

Photonics in nature and bioinspired designs: sustainable approaches for a colourful world

Raquel Vaz, [ID] [abc] Manuela F. Frasco [ID] *[abc] and M. Goreti F. Sales [ID] *[abc]

Biological systems possess nanoarchitectures that have evolved for specific purposes and whose ability to modulate the flow of light creates an extraordinary diversity of natural photonic structures. In particular, the striking beauty of the structural colouration observed in nature has inspired technological innovation in many fields. Intense research has been devoted to mimicking the unique vivid colours with newly designed photonic structures presenting stimuli-responsive properties, with remarkable applications in health care, safety and security. This review highlights bioinspired photonic approaches in this context, starting by presenting many appealing examples of structural colours in nature, followed by describing the versatility of fabrication methods and designed coloured structures. A particular focus is given to optical sensing for medical diagnosis, food control and environmental monitoring, which has experienced a significant growth, especially considering the advances in obtaining inexpensive miniaturized systems, more reliability, fast responses, and the use of label-free layouts. Additionally, naturally derived biomaterials and synthetic polymers are versatile and fit many different structural designs that are underlined. Progress in bioinspired photonic polymers and their integration in novel devices is discussed since recent developments have emerged to lift the expectations of smart, flexible, wearable and portable sensors. The discussion is expanded to give emphasis on additional functionalities offered to related biomedical applications and the use of structural colours in new sustainable strategies that could meet the needs of technological development.

[a]BioMark Sensor Research/UC, Faculty of Sciences and Technology, Coimbra University, Coimbra, Portugal

[b]BioMark Sensor Research/ISEP, School of Engineering, Polytechnic Institute of Porto, Porto, Portugal. E-mail: mffrasco@gmail.com

[c]CEB, Centre of Biological Engineering, Minho University, Braga, Portugal. E-mail: goreti.sales@eq.uc.pt; goreti.sales@gmail.com

1. Introduction

A panoply of astonishing colours is present in nature, derived from chemical and physical phenomena. While the first is based on electronic transitions in molecules that absorb specific wavelengths of visible light, structural colours involve physical processes. Structural colours in nature arise from different mechanisms of light interaction with matter. The

Raquel Vaz completed her BSc degree in Biochemistry in 2017, and her Biomedical Engineering master's in 2019, both from the University of Porto. She is currently a PhD student of Chemical Engineering at Coimbra University. Due to a deep interest in investigation areas such as nanotechnology, biomaterials and nanotherapy, she has been pursuing work at BioMark Sensor Research, aiming to produce biomaterial-based biosensors with great focus on early cancer detection.

Manuela Frasco received a degree in Biochemistry in 2000 and a PhD in Biomedical Sciences in 2007, both from the University of Porto. She is currently a postdoctoral researcher in the BioMark Sensor Research Lab at the University of Coimbra, Faculty of Sciences and Technology, Department of Chemical Engineering. Her main research interests include nanomaterials, biopolymers, biomimetic imprinting, bioinspired photonics and optical sensors.
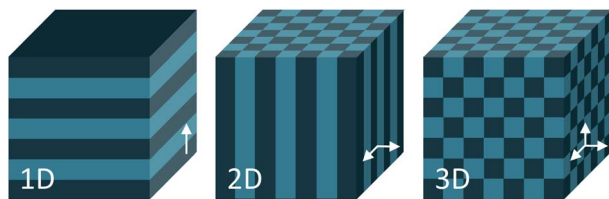
Fig. 1 Schemes of one, two- and three-dimensional photonic crystal structures. The periodic modulation in the refractive index is shown by the arrows.

scattering of light occurs at interfaces between materials of different refractive indexes.[1] Incoherent scattering is responsible for milk-white and blue like sky colours resulting from disordered dispersion of scattering particles.[2] However, when there is a coherent scattering, the constructive interference between scattered waves exhibits colour through enhancement of certain reflected wavelengths.[1,2] Colour from coherent scattering can be produced by the simplest thin-film structures. Thin-film interference occurs when light reflected by both boundaries of a film interfere constructively with each other. This process is strengthened by periodic multilayers of thin-films. Diffraction gratings also have reflective properties due to patterns that repeat periodically with a certain lateral spacing along the surface originating interfering waves.[1,2]

Photonic crystals (PCs) are composed of an array of materials with different refractive indexes, which can have a periodic spatial arrangement in one, two or three dimensions. One-dimensional (1D) crystals consist of a multilayer film of alternating layers of materials with different dielectric constants, whereas the two-dimensional (2D) and three-dimensional (3D) ones are periodic dielectrics in two and three directions, respectively (Fig. 1).[3] The structural colour observed in PCs is expressed by a combination of Bragg's and Snell's laws (eqn (1)) that explains how the angle of incidence of light, periodicity and refractive index affects the reflection wavelength.[2,4]

$$m\lambda = 2d(n_{\text{eff}}^2 - \sin^2\theta)^{1/2} \qquad (1)$$

where m is the diffraction order, λ is the reflected light wavelength, d is the diffracting plane spacing, n_{eff} is the effective refractive index, and θ is the angle of light incidence.

Owing to the periodic modulation of the refractive index, these materials possess a photonic band gap (PBG), thereby certain wavelengths of light are prevented from propagating through the photonic crystal. As a consequence, the crystal reflects the wavelengths located in the PBG, thus, exhibiting vibrant colours if the PBG is within the visible light region.[3,4] A complete PBG is not always realized, and most structures present a pseudo-gap along a certain propagation direction, which does not hamper them to present unique optical properties.[4] This is the case for biological materials and polymers that have relatively low refractive indexes. A wider bandwidth, and hence stronger photonic effects, can be achieved by having greater contrast between refractive indexes. It is possible to achieve higher contrast by controlling the composition and additives, porosity, order and topology, among other parameters, which can be adjusted according to application during nanostructure fabrication.[5,6]

Inspired by many examples of natural structural colours highlighted in the following section of this review, photonic structures with a variety of shapes, length scales, dimensions and materials have been developed (Fig. 2). Several fabrication methods such as lithography, 3D printing, and self-assembly, together with chemical etching techniques can be used to obtain structural colours with diverse functionalities.[7] Attempts to mimic structural natural colours usually rely on colloidal self-assembly of particles, because it is a cost-effective and versatile process. Fabrication methods are based on capillary forces, gravity, assembly assisted by shear, magnetic or electrical

Goreti Sales received a degree in Pharmaceutical Sciences in 1994 and a PhD in Analytical Chemistry in 2000, both from the Pharmacy Faculty of Porto University. She was an adjunct professor in the Polytchenic Institute of Porto, School of Engineering (2006–2019), and currently is an associate professor at Coimbra University. Her research interests are devoted to biomimetic nano-materials and biosensing devices. She is the founder of BioMark, Sensor Research group (2011) and she was awarded a Starting Grant by the European Research Council (2012), targeting a new technical approach that merges biosensors with solar cells. She is currently coordinating the FET-Open project (H2020) MindGAP.
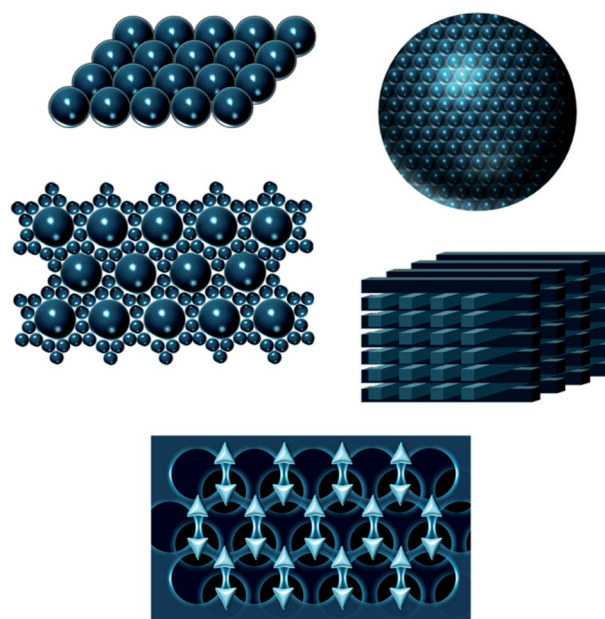

Fig. 2 Schematic examples of bioinspired architectures.

forces. Organized assemblies are easily obtained in close-packed hexagonal, face- and body-centred cubic lattices.[7] Colloidal 3D photonic crystals, like the many examples of opals and inverse opals described in the literature, can be easily modulated according to the application by the use of many types of materials in the structures. Such an ability to tune the system and to improve the spectral resolution is an advantage considering the low costs of fabrication. In addition, using biocompatible and environmentally friendly materials has emerged as a major improvement in this investigation field. Therefore, photonic structures have been recently developed as inverse opals made with biopolymers or by transferring micro and nanopatterns to biopolymers, such as silk,[8,9] zein[10] and chitosan.[11]

It is the dependence of the reflected wavelength on material features, namely periodicity and refractive index (eqn (1)), which makes photonic crystals so interesting to function as sensors in catalysis and bioassays, among many other applications. Photonic crystals can be mechanically, thermally, electrically, magnetically or optically responsive (Fig. 3). These stimuli induce rapid and sensitive changes in the material, usually measurable by a shift in the wavelength and visual colour change.[3] Optical sensors based on photonic structures have been developed to detect a number of molecules of interest.[12] For example, creatinine, cholesterol and organophosphate nerve agents can be enzymatically detected by linking creatinine deiminase,[13] cholesterol oxidase[14] and organophosphorus hydrolase,[15] respectively, to hydrogel-based photonic crystals. These examples and others will be further explored in the forthcoming sections.

Fig. 3 Responsiveness of designed photonic materials to various types of stimuli.

In this review, bioinspired photonic approaches are highlighted in terms of the versatility of materials, structures, fabrication processes and applications. Due to the wide-range of application fields, the main focus is on analytical advantages of using structural colours in biomedical research, while illustrating sustainable, low-cost and cutting-edge technologies to that purpose. Therefore, the review starts by giving insight on structural colours in nature, their underlying mechanisms and fabricating methods to mimic them. Next, promising biomaterials used to build photonic structures are presented, followed by an overview of recent developments on the ability to design smart sensors and to tailor polymeric structures as photonic devices for sensing and diagnostics. Also, related biomedical uses are addressed, namely flexible and wearable devices and image tracking of drug delivery systems. Finally, an outline of other bioinspired applications is given, and future trends in this fascinating and ever-expanding subject to drive innovation in life sciences are summarized.

2. Structural colours in nature

Colours in nature can arise from chemical or physical processes. Chemical colours emerging from light absorbing pigments are explained by the reflectance of selective light wavelengths that they do not absorb, while bioluminescence is the production of light by a chemical reaction within a living organism. Both mechanisms create interesting visual signals for defence, communication and illumination, among other functions used by many biological species.[2,16] As previously mentioned, the focus of this review is on physically originated colours, where the interaction of light with structures whose periodic dimensions of the lattice are in the order of visible light wavelengths result in intense and bright colours that are exempt from fading.[2]

However, it is particularly important to highlight that natural colouration brilliance often arises from combined physical mechanisms (due to nanoarchitecture variants that integrate regularity and irregularity) or cooperative effects between physical structures and pigments.[2,16] Regarding the first phenomenon, nature created patterns of hierarchical structured photonic crystals along with scattering by quasi-ordered and amorphous photonic materials.[17,18] The long-range order of a crystalline structure results in shiny iridescent colours that change with the viewing angle. However, the degree of ordering can be controlled towards amorphous arrays with a short-range order. The amorphous structures, also named photonic glasses, have reduced iridescence and lower angle dependency in comparison to colloidal crystals due to the irregularity of the structures.[17,18]

Materials found in nature, which are used for optical effects – colouration, camouflage, protection against radiation, vision and photosynthesis – include chitin, keratin, cellulose, guanine, reflectin, aragonite and collagen. Regarding photonic structures, cellulose, chitin and keratin are the most prevalent biomaterials.[16] For example, the iridescence blue colour of fruit *Pollia condensata* and of the leaves of Malaysian plants arise from helicoidal cellulose structures,[19,20] while the colours of
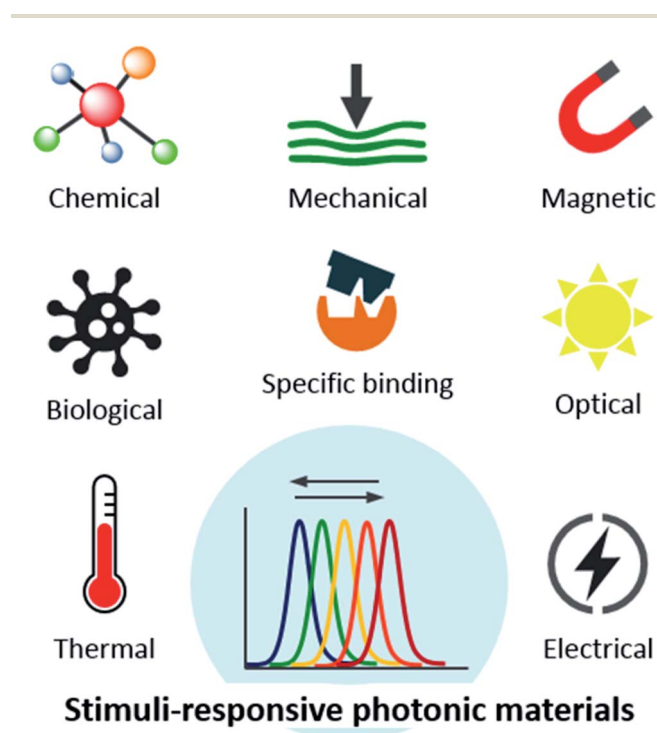
scarab beetles and butterflies' wings derive from chitin nanostructures[21–23] and those of peacock feathers from melanin rods connected to keratin.[24]

Structural colouration due to photonic crystals has evolved in major biological groups and can be found in both terrestrial and aquatic systems, being more abundant in animals. In plants, the usual roles of structural colours are to make them more attractive for insects and birds, as defence against herbivores, for ultraviolet (UV) light protection and to increase the capture of photosynthetically important wavelengths.[20] For example, the fruit of *Pollia condensata* is unique among the family of Commelinaceae found in the African forest, as well as regarding the remaining flora, because it shows a metallic blue color with a pixelated appearance (Fig. 4A). The cell walls are composed of photonic helicoidally stacked cellulose microfibrils, emitting a dominant intense blue colour caused by Bragg reflection. The pointillist aspect is due to differences in layer thicknesses of the multilayer stack from cell to cell, thus the reflected colour is also different.[19] Fruits of *Elaeocarpus angustifolius*[25] and *Delarbrea michieana*[26] also present blue iridescence due to cellulosic structures in the epidermal cells beneath the cell wall.

In 2005, Vigneron *et al.* showed that the *Leontopodium nivale*, a European alpine flower, exhibits white filamentary surfaces that have the main aim to protect the plant from cold, UV light and dehydration. The collection of fibres can be described as a 2D photonic structure that absorbs UV light.[27] More recently, Diah *et al.* (2014) studied the colouration of Malaysian plants,

which exhibit an iridescent blue colour on their leaves. The colouration of the herbs *Mapania caudata*, *Diplazium crenatoserratum* and *Phyllagathis rotundifolia* arises from biogenic silica nanoparticles.[20] Particularly, in the case of *Mapania caudata*, its structural colour is based on helicoidal cellulose and a layer of silica nanoparticles present in the epidermal cell wall.[28] However, a helicoid morphology causes iridescence only with circularly polarized light of the same handedness as that of the helicoid morphology. This is not observed when the iridescence is caused by periodic variation of the refractive index of multilayers instead of helicoidal structures, like in two species of *Phyllagathis* and Asian begonias.[28]

Regarding animals, many present structural colours, from the smallest insects and arachnids to birds and chameleons. Colouration and the change of its hue is often used for camouflage, sexual selection and warning predators.[29]

Photonic crystals arranged in 1D are usually present in insects, like the multilayer structures responsible for the metallic colours of many jewel beetles. The cuticles of *Chrysochroa fulgidissima*, the Japanese jewel beetle, have layered microstructures consisting of alternating layers with different refractive indices and thicknesses, namely chitin and melanin. In addition, under high incident angles, the light reflected by these photonic structures is strongly linearly polarized, which is quite interesting as insect eyes can detect polarized reflections and this may be a mechanism for each other's recognition.[30] In contrast, for jewel scarab beetles, circular polarization is a predominant feature determined by the helical structure of the stacked chitin nanofibrils. The vivid golden and silver reflections of jewel scarabs of *Chrysina* genus (Fig. 4B) result from combining chirped multilayer structures, *i.e.*, spatial periods that gradually change along the cuticle's depth, with a chiral helical arrangement of the nanofibrils and uric acid crystallites embedded in the matrix.[21]

In the case of butterflies, the photonic crystal is more complex because it has structural variations within the layers of the multilayer structures present in the ridges of wing scales.[22,31] Particularly, in the case of *Morpho* butterflies, the uniform vivid blue reflection can be attributed to a combined interference and diffraction of light, together with pigmentation. The lamellar structure within a ridge exhibits constructive interference, while the narrow width and the irregular height of a ridge cause light diffraction. The pigmentation serves to enhance the blue colouring.[31] The wing scales of other butterfly species that show bright signalling colours have also been studied. The green and violet colours on the wings of *Sasakia charonda* and the *Euploea mulciber* originate from a tilted multilayer cuticle-air arrangement on the ridges forming a 3D lattice, which is similar to the one found in *Ancyluris meliboeus*. The iridescence of *Chrysozephyrus ataxus* results from multilayers in the groove plates between the ridges and ribs which also reflect violet and green wavelengths.[23] Other examples include the *Cyanophrys remus*, *Callophrys rubi*, *Parides sesostris* and *Teinopalpus imperialis* butterflies, which owe their colour to gyroid structures having a body-centred cubic air-cuticle 3D lattice.[22]

The Australian peacock spiders *Maratus robinsoni* are quite interesting because they are able to display the full-spectrum of
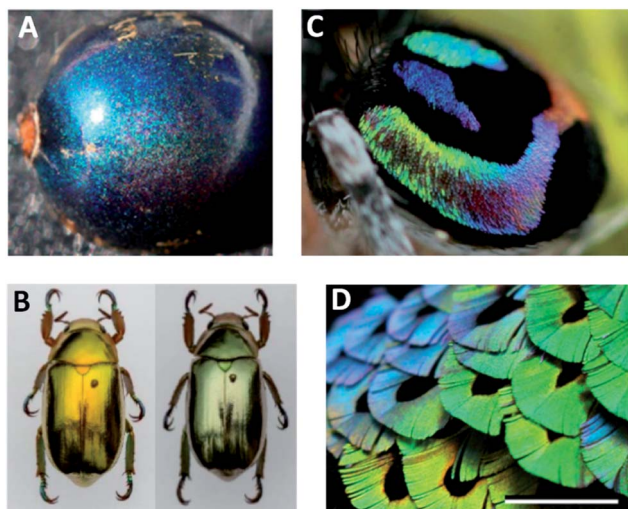
Fig. 4 Naturally occurring bright iridescent colours: (A) Iridescence of a single fruit of *Pollia condensata* (reproduced with permission.[19] Copyright 2012, National Academy of Sciences); (B) metallic-like reflection colours of golden-like and silver-like *Chrysina chrysargyrea* jewel scarabs (reproduced under the terms and conditions of the Creative Commons Attribution (CC-BY) License.[21] Copyright 2018, The Authors, published by MDPI); (C) miniature peacock spider *Maratus robinsoni* with rainbow-iridescence (reproduced under the terms and conditions of the Creative Commons Attribution (CC-BY) License.[33] Copyright 2020, The Royal Society of Chemistry); (D) breast feathers of bird-of-paradise Lawes's parotia, *Parotia lawesii*, scale bar 1 cm (reproduced with permission.[34] Copyright 2014, National Academy of Sciences).

iridescent colours in an angle-dependent way. These arachnids use colour during courtship, showing their amazing abdomen to attract mates. The hue modification is caused by 3D airfoil-shaped nanograting scales and an underlying black cuticle layer (Fig. 4C). The scales enhance the power of the diffraction grating, while the black layer absorbs background scattering allowing brighter colours.[32,33]

The feathers of birds display intense colours with well-studied biological purposes. The red, yellow and black colours can be assigned to the presence of pigments, but intense reflections usually indicate the existence of quasi-ordered nanostructures constituted by keratin, melanin and air.[29,34] The bird-of-paradise Lawes's parotia performs ritualized dances to attract mates while displaying coloured feathers, especially the barbules of the breast (Fig. 4D). These feathers contain a multilayer of melanosomes in a keratin matrix that are densely packed and arranged in a boomerang-shaped cross-section. This morphology allows 3D reflections and a colour switch.[34]

In another example, the male peacock tail presents an extraordinary diversified pallet of iridescent colours: blue, green, yellow and brown. These colours derive from very similar 2D photonic crystals consisting of melanin rods connected by keratin (Fig. 5).[24,35] Nonetheless, while the blue, green and yellow barbules have a nearly square lattice, the brown one is rectangular. They also differ in the rod spacing (related to the lattice constant) and in the melanin rod layers (related to the number of periods of the photonic crystal). The number of periods controls the generation of additional colours and by varying the lattice constant, the frequency of the partial PBG shifts, which explains the different colours of the feathers.[24]

Other birds, such as ducks, also present iridescent colours. In duck barbules, the colour arises from a photonic hetero-structure composed of a 2D hexagonal lattice of rod-shaped melanosomes embedded in a thin layer of keratin.[29] This close-packed hexagonal configuration is so energetically stable, that the photonic crystal is likely achieved by a self-assembly process. Through variations in size and spacing between melanosomes, duck feathers obtain colours ranging from violet to red.[29] The common magpie (or black-billed) has a plumage that looks black and white. However, the dark areas of the wings show blue iridescence, and its tail is yellowish-green with a blue termination. The colours found in the barbules of feathers also derive from the hexagonal 2D lattice of keratin and melanin containing cylindrical air channels.[36]

As mentioned, reversible changes in the structural colours offer camouflage properties. An appealing example is the colour change on chameleons, thought to be due to the dispersion or aggregation of pigment-containing organelles, as it happens with other vertebrates. However, it was shown that it is not such a simple process, because nanophotonic crystals are involved (Fig. 6). The skin of panther chameleons is composed of two layers of iridophore cells, which contain guanine nanocrystals. Their sizes, form and organization differ between the two layers. The upper layer is responsible for a fast change of colour through alteration of guanine spacing to a triangular lattice. The second layer improves resistance to thermal changes resulting from sunlight exposure through reflection of near-infrared light.[37]

Even though in less number, it is also possible to find some examples of aquatic organisms whose colour depends on photonic crystals. For example, the worm *Pherusa* sp. setae exhibits a strong colour due to a 2D photonic structure, which is constituted by hollow cylindrical channels packed hexagonally.[38] Moreover, diatoms, which are unicellular microalgae found in diverse freshwater and marine systems, also possess iridescence in the frustule, a cell encasement, derived from
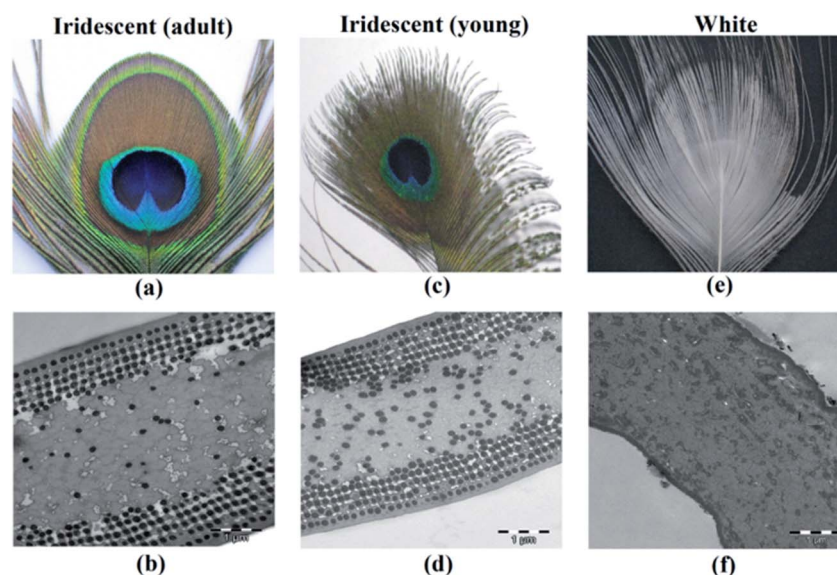

Fig. 5 Photograph (a) and TEM image (b) of adult peacock feathers showing iridescence; photograph (c) and TEM image (d) of young peacock feathers; and photograph (e) and TEM image (f) of a white peacock feather. White feathers lack melanin rods, thus the colour is due to scattering in the keratin matrix. The adult and young brown barbules show 2D photonic crystals, but with different rod spacings (lattice constant) (reproduced with permission.[35] Copyright 2015, OSA Publishing).
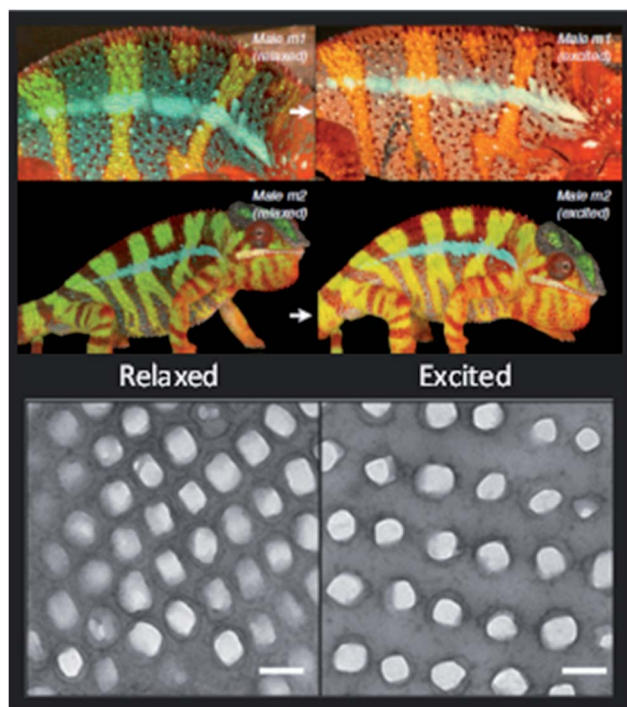
Fig. 6 Reversible colour change of two male chameleons while passing from a relaxed state (left column) to an excited state (right column), with the respective TEM images of the guanine nanocrystal lattice in S-iridophores in the two states (scale bars 200 nm) (reproduced under the terms and conditions of the Creative Commons Attribution (CC-BY) License.[37] Copyright 2015, Springer Nature).

periodic nanoporous structures of biosilica. Diatoms use these structures to focus the optimal light wavelengths for photosynthesis on the chloroplasts distributed in the cell surface.[39] It is also possible to find a complex 3D structure in the *Cystoseira tamariscifolia* brown algae, which is an opal-like photonic structure made from lipids and found intracellularly close to chloroplasts (Fig. 7). Although its function is still unknown, it may have a role in photosynthesis.[40] Another example is the fish *Paracheirodon innesi* that possesses periodically stacked platelets of guanine crystals in skin cells that exhibit a cyan colour. This colour rapidly changes to yellow under stressful conditions due to a change of platelet angle.[41]
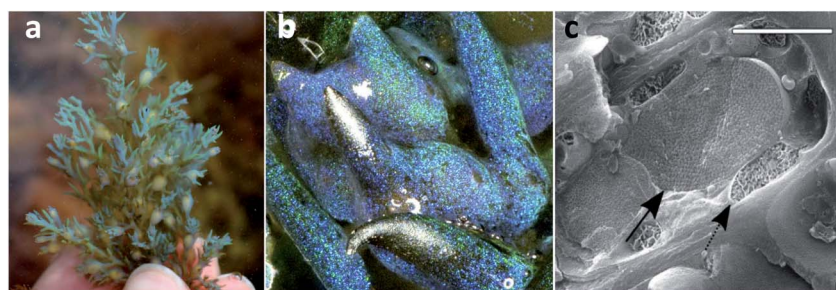
3. Fabrication methods to mimic nature's photonic crystals

Photonic crystals found in nature proved to be interesting and smart optically active nanostructures. Their mimicry for scientific and technological applications, such as for sensor improvement, enhancement of solar cells and communication technologies, has been showing incredible potential and success. Furthermore, recent advances in nanotechnology defined a new era of enormous flexibility in material composition, choice of lattice periodicity, symmetry and introduction of defects within the photonic structures.[42]

The fabrication of PCs may rely on top-down methods, which uses lithography to fabricate nanostructures from an initial bigger piece of material. For example, electron-beam lithography (EBL) scans a focused beam of electrons to shape the resist (an electron-sensitive film) into periodic nanostructures (Fig. 8A). It has the advantage of not needing a mask as other lithography techniques, since it is possible to directly write the pattern onto the substrate.[43] This technique allows obtaining structures with less than 10 nm and with an alignment accuracy of less than 50 nm.[44] Belotti *et al.* (2004) used EBL to obtain 2D photonic triangular lattices on a silicon-on-insulator wafer, where modulating the doses of the electron beam enabled to precisely obtain hole diameters ranging from 250 to 465 nm.[45] Later, layer-by-layer stacking with EBL became more frequent, since it enabled to obtain uniform 3D structures with a versatile design: Subramania *et al.* (2004) fabricated a five-layer 3D woodpile photonic crystal with a PBG in the infrared spectrum,[46] while Wang *et al.* (2009) achieved a face-centred-tetragonal woodpile photonic structure with a superprism effect also in the infrared spectrum.[44] A major challenge with EBL is the patterning of large areas (in order of millimetres), while maintaining accuracy, but Bonam *et al.* (2016) achieved it through dose control of the electron beam, penetration depth of high energy electron beams ($\geq$100 keV) and tailored photoresist tones and contrasts.[47] It is also worth mentioning that EBL can be used to add defects within the PC, in order to manipulate the PBG (Fig. 9A).[48] A more thorough review on nanofabrication by EBL and its applications can be found in the work by Chen *et al.* (2015).[49]

Fig. 7 Photograph of *C. tamariscifolia*, showing structural colour (a), low-magnification image of the specimen (b), and a cryo-SEM image of an epidermal cell, showing the photonic structure (solid arrow) and a chloroplast (dashed arrow) (c). Scale bar of 2 μm (reproduced under the terms and conditions of the Creative Commons Attribution (CC BY-NC) License 4.0.[40] Copyright 2018, American Association for the Advancement of Science).
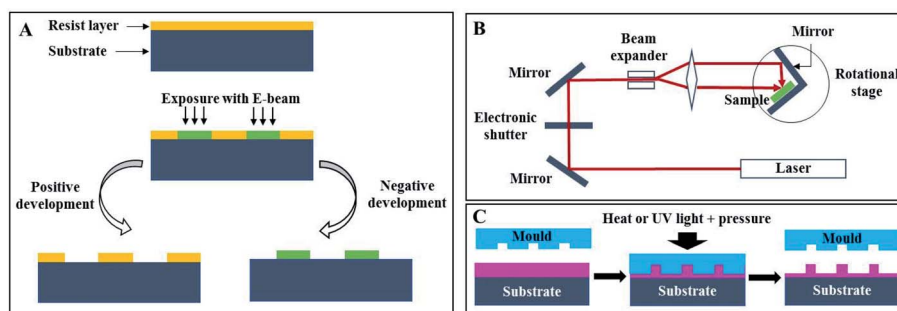
Fig. 8 Schematic representation of different lithography techniques: (A) electron-beam, (B) holographic and (C) nanoimprint.

Even though EBL can be used to obtain 3D structures, it is usually used to produce 1D and 2D ones, because more than that requires multiple stacking by precise alignment between different layers, which is time-consuming. Holographic lithography (HL), also denoted as multi-beam interference lithography, is more economical and needs only one single step to achieve larger areas and volumes. The basic principle of HL is the interference between two or more coherent electromagnetic waves, which is recorded in a resist (Fig. 8B). The split of coherent light into several beams prior to their recombination is achieved by a reflective optical element, a phase mask or a single prism.[50] When using multiple exposure 2-beam interference, it was possible to create 3D PCs, by assembling multiple 1D or 2D structures.[51] Photonic arrays built with HL were already studied for numerous applications, for enhancement of Raman spectroscopy,[52] and as gas sensors[53] and optofluidic lab-on-a-chip[54] (Fig. 9B).

As previously observed, HL is a one-step method employed to fabricate large size and periodic PCs. However, it has the drawback of not being able to simultaneously introduce defects while fabricating PCs, therefore those defects are later introduced *via* laser writing or multiple exposures. A phase-controlled HL technique was developed for overcoming this problem, where each interfering beam is controlled using a phase mask for multi-beam diffraction.[55,56] Nowadays, a spatial light modulator is generally used for creating defects or for engineering more flexible designs.[57–59]

Nanoimprint lithography (NIL) is a technique where the nanopattern present on a stamp originally made by EBL is transferred by employing pressure and temperature (Thermal NIL, also known as hot embossing), or pressure and UV light (UV NIL) against a polymer (Fig. 8C), which may then be used as an optical waveguide itself or as a resist for pattern transfer to another substrate.[60] NIL overcomes the EBL limitation of not being suitable for mass production, besides being a cost-efficient approach, marked by choice variety regarding polymers, provided that they enclose high transmission and an adapted refractive index.[60,61] Choi *et al.* (2006) used the synthetic polymer polystyrene (PS) for replication of a 2D PC with a triangular array of holes.[62] Other examples include imprinting the PC into a light emitting diode (LED) substrate[63] or into a poly(methyl methacrylate) (PMMA) layer.[64] The use of natural polymers of silk[65] and cellulose[66,67] has been also explored, which opens a new perspective into optical biocompatible devices. Of note is also attaining PCs in non-planar surfaces, such as lenses.[68]

Even though lithography allows better control, it remains a time-consuming and expensive technique, compared to
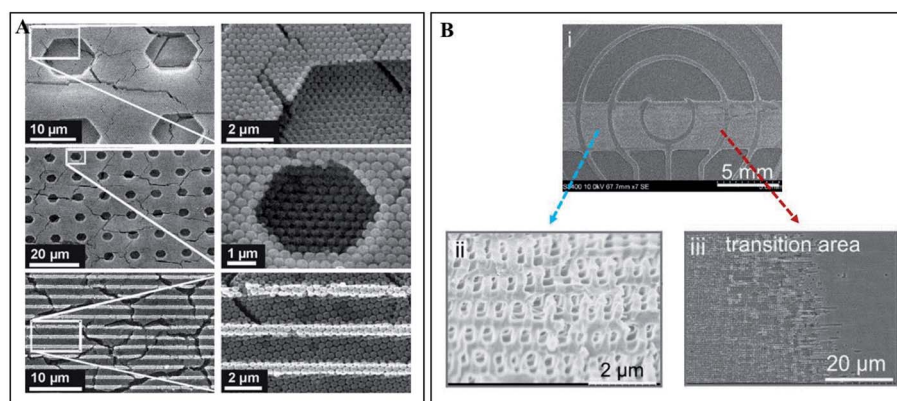

Fig. 9 (A) SEM images of defects (hexagonal and straight parallel trenches) fabricated in a 3D opal photonic crystal by electron-beam lithography (reproduced with permission.[48] Copyright 2004, Elsevier); (B) optofluidic device fabricated by holographic lithography (i), where the photonic structure is visible (ii) formed against solid photoresist walls (iii) (reproduced under the terms and conditions of the Creative Commons Attribution (CC-BY) 4.0 License.[54] Copyright 2016, Nature).
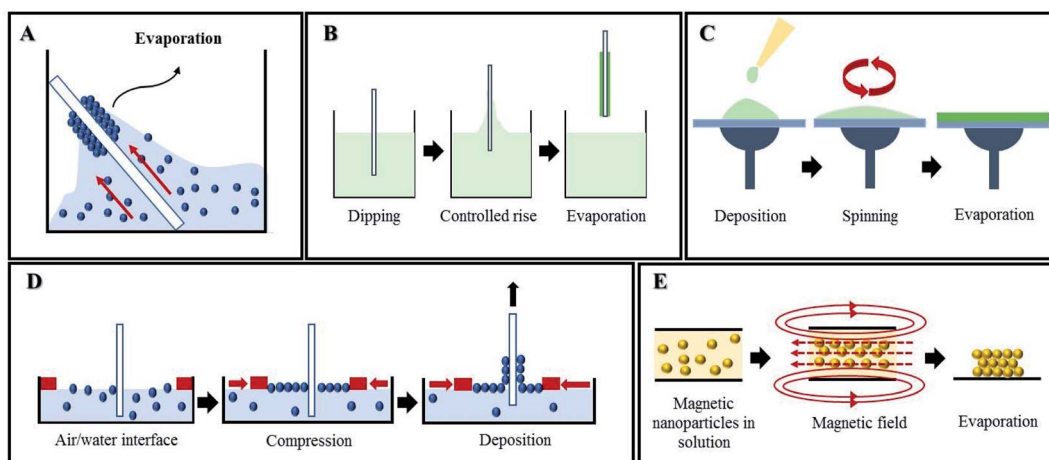
Fig. 10 Self-assembly methods for PC fabrication: (A) vertical deposition, (B) dip-coating, (C) spin-coating, (D) Langmuir–Blodgett and (E) magnetic assembly.

bottom-up approaches, which have been gaining considerable attention, since they only depend on the self-assembly of building blocks (usually silica, PMMA or PS nanoparticles) into a photonic lattice, resulting in a faster and cheaper method.[42] Self-assembly methods also have great popularity, due to flexibility in materials choice and purposes. Moreover, most self-assembled PCs have face-centred-cubic or hexagonal-close-packed stacking.

A very simple method of self-assembly is drop-casting, wherein a drop of colloidal suspension is spread on the desired substrate and allowed to evaporate, which pulls the nanoparticles together.[69,70] Evaporation is also the main characteristic in the vertical deposition method, where a substrate is vertically submerged in a colloidal solution and allowed to evaporate for several days (Fig. 10A). Besides simplicity, it also allows having more control over the parameters to fabricate multi-layered photonic structures than drop-casting.[71,72] Vertical deposition opens up new designs like binary PCs by using nanoparticles with different sizes (Fig. 11)[73] and also functionalized PCs, such as with fluorescent probes.[74] The use of this technique is illustrated in a new method engineered for polyester fabric colouration, without the use of chemical dyes and pigments, which decreases pollution during the process.[75–77] Another practical example is the development of an optical biomedical biosensor for venous thromboembolism detection, based on a photonic molecularly imprinted polymer.[78] Nonetheless, vertical deposition is time-consuming and any interruption in the process affects the quality of the crystal. Another widely used method relying on control over the rate of solvent evaporation is dip-coating, where a substrate is vertically held and submerged into a colloidal suspension, being slowly pulled up (Fig. 10B). Therefore, by controlling the speed of this process, it is possible to control the layers' thicknesses[79] and prepare PCs whose layers are composed of different materials[80] or from core–shell nanoparticles to obtain new characteristics.[81] Dip-coating is faster than vertical deposition, needing only a few hours, but uniformity is difficult to maintain.[42]

Centrifugation and spin-coating depend on centrifugation forces, where the colloidal suspension is centrifuged at high speeds to bring the particles together. The quality of the PC depends on the colloidal concentration, the solvent used, centrifugation time, velocity and temperature.[82,83] Spin-coating is a fast and facile mechanism for producing thin uniform mono or multi-layered photonic films by rotation of a horizontally oriented suspension, therefore the PC forms due to evaporation (Fig. 10C).[84] It can not only be used to obtain large-scale PC assemblies,[85,86] but also macroporous polymers and polymeric nanocomposites,[87] as well as creating defects[88] and to build structural templates to pattern silicon substrates.[89]

Other techniques for fabricating PCs have been developed in order to allow more precise and accurate control than the aforementioned ones. The Langmuir–Blodgett (LB) method is a strong candidate for that purpose, since monolayers of
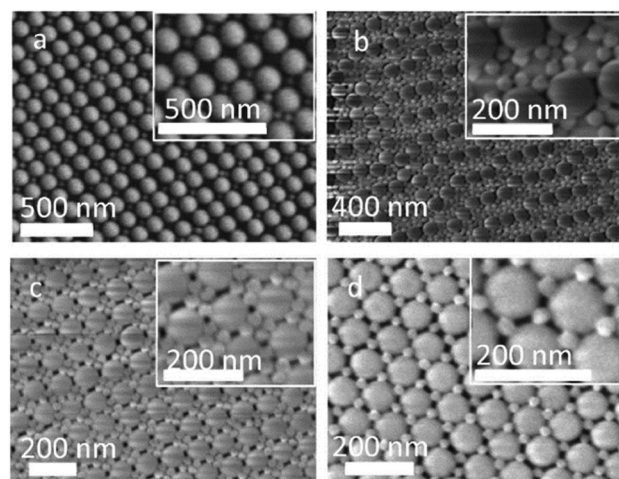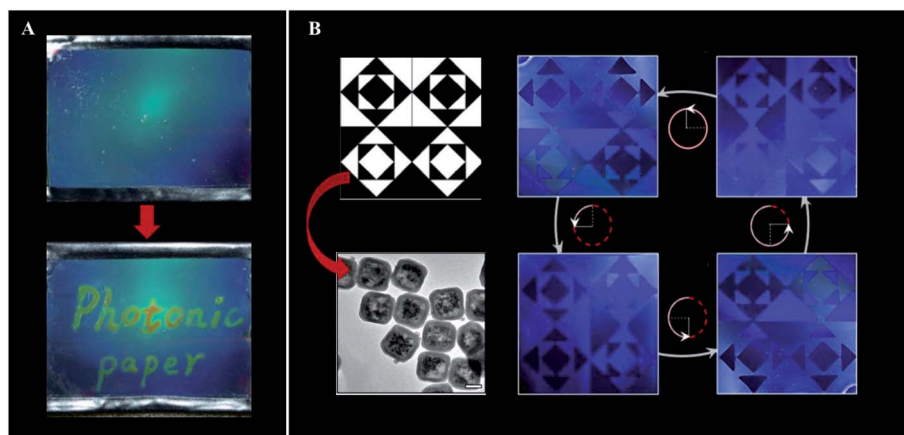

Fig. 11 Binary photonic crystals grown by vertical deposition using silica nanoparticles with different sizes; the images show the versatility of design with this method of fabrication (reproduced with permission.[73] Copyright 2017, American Chemical Society).

Fig. 12 Examples of application of magnetic oriented photonic crystals: (A) photonic paper prepared through the magnetic field–induced self-assembly of Fe_3O_4@SiO_2 colloids, followed by a simultaneous UV curing process to fix the photonic structures inside the PEGDA matrix. The "ink" is a hygroscopic salt solution that creates durable contrast of diffraction colours on the paper (reproduced with permission.[104] Copyright 2009, Wiley VCH); (B) Fe_3O_4@SiO_2 nanocubes (TEM image, bottom left) were fixed with a vertical and horizontal alignment in the dark and white regions, respectively, to create an encryption film. The blue images correspond to the printed pattern under the same light illumination, but with counterclockwise rotation from 0° to 270° (reproduced with permission.[106] Copyright 2019, American Society of Chemistry).

nanoparticles are compressed on a water surface (Fig. 10D) and subsequently transferred to another substrate by mobile arms to obtain multilayer structures with the desired parameters. Despite the two steps needed in LB, none of the self-assembly methods described above can match the high level of flexibility regarding particle size and composition and ultimate PC design achieved using LB.[90,91] LB can also be used in coordination with other techniques aiming for the creation of a defect within the PC. For that, a layer of nanoparticles with different sizes is introduced in-between similar multilayers of the PC.[92,93] LB has already proved successful with non-planar substrates, which opens up future possibilities for research and commercial applications.[94]

Another simple, rapid and inexpensive technique that enables the preparation of large-scale colloidal PC films is spray-coating. The colloidal suspension is inserted in an air spray gun, and upon air pressure, the suspension is ejected towards the substrate. This method is very versatile, enables printing precise patterns and can be successfully used in several substrates, including flexible ones (*e.g.*, paper, plastic, fabrics).[95,96] As for other methods, there are important parameters that have to be optimized, namely the viscosity of the dispersion and the wettability of the substrate.[97]

Magnetic self-assembly is an interesting method that drives paramagnetic colloidal particles to assemble under the effect of an external magnetic field (Fig. 10E). The application of the magnetic field creates 1D chains between particles, due to interparticle attraction; the interparticle separation is defined by the balance between attraction and repulsion forces.[98] It is also possible to assemble non-magnetic particles into PCs with this technique, as long as they are modified with magnetic materials[99–101] or get resuspended in nanocrystal-based ferrofluids.[102] Implementation of magnetic PCs was already studied for humidity sensors,[103] photonic paper and ink (Fig. 12A),[104] and anti-counterfeiting labels (Fig. 12B),[105,106] among others.

Instead of using a magnetic field, colloidal suspensions can be arranged by the influence of an electric field, whose main advantage is controlling the thickness of the film, since it increases proportionally to the amount of electric charge.[107] However, in this technique, a nanostructured substrate is usually used as a template to imprint other materials growing within them by applying an electrical field.[108] For example, Liu *et al.* (2012) used a PS template to achieve an electrodeposition of 3D ordered macroporous silicon films from an ionic liquid.[108] Template-assisted electrodeposition of transition metal oxides has been also pursued for optical coatings, since they possess excellent optical properties, such as high transmittance, high refractive index, and high hardness and thermostability.[109–112] Another technique based on the application of a potential is electrospinning (ES), which involves a polymer solution in a capillary at a higher voltage than the deposition plate. Because of the electrostatic force developed, polymer fibres are deposited. Photonic fibres have great potential for light generation and collection in electronic devices. However, ES has limitations, due to instability during the chaotic motion of the depositing fibres, and not all polymers are amenable to be used.[113]

Although there is a wide range of choices regarding mechanisms to obtain PCs whose structure allows properties similar to the ones found in nature, it is still important to increasingly substitute synthetic materials for biomaterials, to assure their biocompatible and non-toxic applications. This topic will be reviewed next.

4. Photonic biomaterials

In a world with increasing awareness regarding the environment, new optical techniques using photonic biomaterials have been developed in the last few years, owing to their inherent biocompatibility and biodegradability features. Among the many
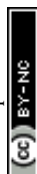
applications, some may be highlighted, like therapy, diagnostics, sensing and imaging fields. To achieve the full potential of photonic biomaterials, their availability in the ecosystem and optical, mechanical, chemical and biological properties must be considered. In particular, polysaccharides, such as cellulose and chitosan, as well as the proteins silk and zein, are promising biopolymers for optical purposes.[114] Cellulose is the most abundant polymer in nature, being usually extracted from plants. It is found as fibres, but after mechanical or chemical treatments, it is possible to obtain cellulose nanofibrils or nanocrystals.[66] A mesoporous chiral cellulose membrane with photonic properties was constructed by Giese *et al.* (2014). Changes regarding pressure and solvent polarity affected the colour of the membrane thus allowing naked-eye detection (Fig. 13).[115] Nitrocellulose is cellulose modified with a nitrating agent such as nitric acid, and it has also been used to form photonic biopolymers. Paper-based microfluidic chips were built with a nitrocellulose inverse-opal, and showed to be responsive to the presence of human IgG.[116] If cellulose is modified to get hydroxypropyl cellulose, it presents iridescent colours and chirality in concentrated solutions. However, optical functionality can also be obtained from such cellulose derivatives using alternative methods. Espinha *et al.* (2018) used hydroxypropyl cellulose to obtain free-standing membranes through nanoimprinting. This convenient soft lithography approach enabled the obtaining of various morphologies and topographies that were successfully demonstrated as photonic papers and plasmonic substrates to enhance the Raman signal.[66]

Chitin can be found on the exoskeleton of arthropods and cell walls of fungi, in the form of semi-crystalline nanofibres. Chitin is insoluble in water and common organic solvents, so it is usually deacetylated to form chitosan, whose amino groups allow it to be soluble in acidic solutions (pH < 6.5). Both chitin and chitosan are analogues of cellulose, since they all have a repeated β (1 → 4) linked-D-glucose unit.[117] Chitosan has been the most studied biopolymer in the application of photonic structures. It is known to be easily obtained from natural sources, as well as by its biocompatibility, biodegradability and edibility.[11] Huang *et al.* (2014) used PS nanoparticles and chitosan to form a 3D face-centred-cubic inverse-opal photonic structure to detect different organic solvents. The response to organic solvents leads to changes in the structural colour thus, allowing a fast and naked-eye perception of which solvent was present.[11] Nguyen *et al.* (2016) also developed a photonic nanomaterial based on chitosan to detect different solvents. In this study, chitosan nanofibrils were obtained through an alkali treatment of discarded crustacean shells composed of chitin. These nanofibrils were then used to form a hydrogel, whose swelling in the presence of different solvents leads to a colour change (Fig. 14).[118] Ryan *et al.* (2016) explored the response of a composite hydrogel made of ordered silica nanoparticles and a polymer network of chitosan and tetraethylorthosilicate, with suitable flexibility and mechanical strength. The obtained photonic membrane was responsive to pH due to its swelling ability and has numerous anticipated applications in sensing.[119] More recently, Chen *et al.* (2018) engineered a new system of
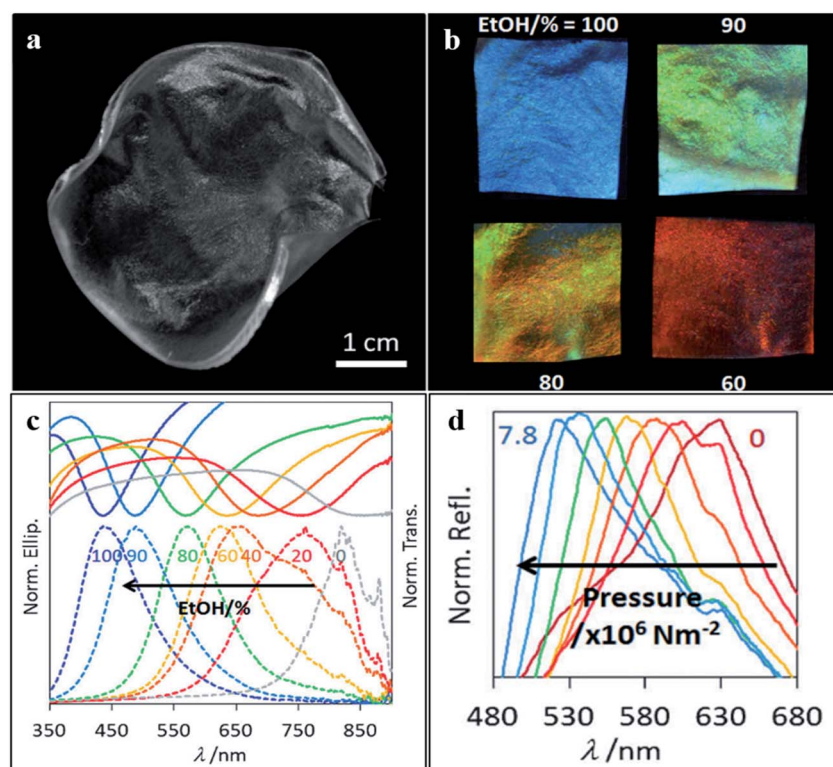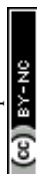

Fig. 13 Photograph of the cellulose membrane (a) used to detect changes regarding (b and c) solvent polarity and (d) pressure, which can be detected by the naked eye (reproduced with permission.[115] Copyright 2014, Wiley-VCH).
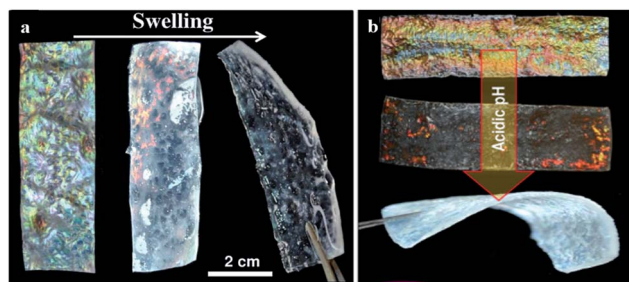
Fig. 14 Photonic hydrogels by swelling of acetylated chitosan nano-fibrils (a), and made of mesoporous chitosan nanofibrils and PMMA composites that show a change in colour to red and transparent during swelling in acidic media (b) (reproduced with permission.[118] Copyright 2016, Wiley-VCH).

drug release for wound healing, based on a chitosan inverse opal, whose interconnected pores could carry the fibroblast growth factor (FGF) encapsulated in a thermo-responsive hydrogel. The release of the FGF cargo was triggered when temperature increased at the inflammation site, and it was monitored by a blue-shift of the reflection peaks of the composite inverse opals.[120]

Silk is a natural protein fibre produced by silkworms, moths, butterflies and spiders. It is biocompatible and biodegradable thus, it has been emerging as a promising approach in the biophotonic and biosensor fields. By casting a silk solution into a colloidal crystal and after removal of the nanoparticles, an inverse opal responsive to the humidity level is obtained.[8] Min *et al.* (2017) went further by using a silk hydrogel inverse opal to engineer an ocular prosthesis, whose opalescence and mechanical properties could be precisely tuned.[121] Silk has also been used to form an inverse opal to sense protease activity in cell cultures, which can be achieved *in situ* and detected through structural colour gradual disappearance.[122]

Zein is a corn protein with interesting properties as a biopolymer. Since it has both hydrophobic and hydrophilic groups, its properties can be tailored according to the contact surface during self-assembly.[123] It has been shown that by direct transfer of gold or silver nanostructures to zein, there was replication of various nanophotonic patterns, like nanopores, nanopillars or pyramid structures. Moreover, the zein photonic nanostructures were shown to enhance the Raman signal of rhodamine 6G.[10] Gold coated zein films with nanophotonic properties have also been successfully produced by replication of poly(dimethylsiloxane) (PDMS) moulds covered with gold. The films were used to detect the peanut allergen Ara h1, using surface-enhanced Raman spectroscopy (SERS).[124]

Even though polydopamine is a synthetic polymer, it can also be included in the list of photonic biomaterials, since it derives from dopamine, a melanin related polymer. Natural melanins can be found in several organisms, such as bacteria and fungi, to protect them from cell damage due to light, temperature and chemical stresses. It is also present in the ink of cephalopods, with the aim of defence against predators, and in humans (*e.g.*, in the skin, hair, eyes, inner ear), among many other examples in nature with diverse functions and properties.[125] Polydopamine is generally used to enhance the vivid colours of photonic crystals. In nature, melanin granules contribute both as components of structural colours and as light-scattering absorbers.[126] Many examples in the literature try to fine-tune structural colours by controlling four variables: size, arrangement, blackness and refractive index. This has been achieved by using PS nanoparticles with a shell of polydopamine to produce crack-free crystals with iridescent or non-iridescent colours, according to the thickness of the shell, the core diameter and order-disorder hierarchy (Fig. 15).[126–129] Moreover, it is also possible to use polydopamine itself to produce nanoparticles, which can then be altered with polymer brushes, namely the hydrophilic poly(2-hydroxyethyl methacrylate) (PHEMA). The photonic materials presented non-iridescent colours, and the colour arising from hairy particles was different, in agreement with increased distance between particles. Thus, by grafting the particles with polymers of different lengths it is possible to easily change the structural colour and obtain functional materials.[130]

There are already some applications of core–shell nanoparticles using polydopamine for the development of advanced optical devices. Zhu *et al.* (2016) developed a polydopamine Janus film through the polymerization of dopamine under alkaline pH at the surface of a water-exposed 2D array of PS nanoparticles. After removal of the nanoparticles, the film worked as a femtolitre cup array, which demonstrated excellent properties for SERS by further modification with silver nanoparticles.[131] In addition, polydopamine coated silica nanoparticles were used to construct photonic barcode beads with the ability to immobilize biomolecules. Subsequently, an immunoassay was developed to detect tumour markers, namely alpha fetal protein, carcinoembryonic antigen and prostate specific antigen.[132] In another study, a polydopamine film was obtained using a layer-by-layer deposition, and further decorated *in situ* with spherical gold nanoparticles. Such a promising plasmonic material was successfully used to detect the content of sugars in beer wort through Localized Surface Plasmon Resonance.[133]

5. Smart structural colour-based sensing polymers

Optical photonic sensors have been extensively studied to identify physical, chemical or biological changes in the medium of interest. Owing to the ability of tuning these systems to reflect light in the visible spectrum, the colour changes can be identified by the naked eye and no complex apparatus for reading the signal is needed.[134] Colorimetric responses in photonic sensors result in blue or red shifts of the observed reflectance. Through these variations, photonic crystal-based devices can be utilized for vapour, solvent, temperature, pressure, pH, ionic strength or biomolecule sensing.[134] Creating sensing devices usually involves polymers, since they are versatile and can be modified for different applications. Indeed, the possibility of modifying the polymer network with functional molecules (*e.g.*, antibodies, aptamers, enzymes) can greatly improve the recognition ability of the photonic polymer sensor.[135]
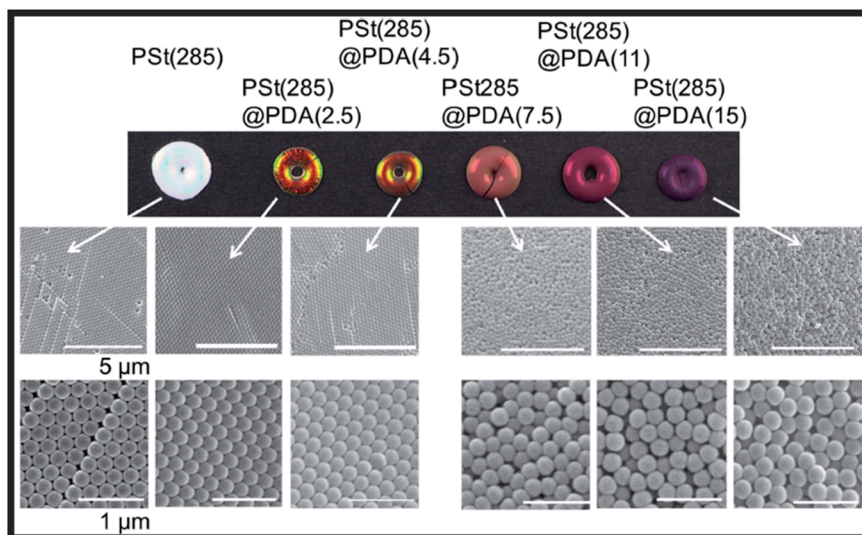
Fig. 15 Images of iridescent and non-iridescent structural colours obtained from core particles of polystyrene of 285 nm, PSt(285), with a shell of polydopamine (PDA) of increasing thicknesses; the respective SEM images show the transition from ordered arrays (iridescent) towards amorphous structures (non-iridescent) by controlling the thickness of PDA (reproduced under the terms and conditions of the Creative Commons Attribution (CC-BY) License.[126] Copyright 2016, The Authors, published by Springer Nature).

Research on "smart polymers" has been intensified because of their ability to respond to environmental changes, such as temperature, pH, mechanical stress and ionic strength. One of the most studied classes of smart polymers is that of hydrogels.[136] Photonic hydrogels are usually 3D polymer networks that either encase periodically packed colloidal arrays or have an ordered porous polymer matrix after etching away the precursor colloidal particles. They can be sensitive to a certain analyte, producing a physical or chemical change most commonly translated into a volume change, which in turn alters their optical properties (Fig. 16).[137]

They are very useful for sensing carbohydrates, as in the case of polyacrylamide (PAAm), PAAm-poly(ethylene glycol), or PHEMA hydrogels, containing an array of colloidal particles or an inverse opal structure, and functionalized with boronic acid groups as recognition elements for glucose binding.[138–140] In terms of detecting solvents, pH, temperature and ionic strength, many examples in the literature can be found presenting different photonic crystal fabrication approaches and
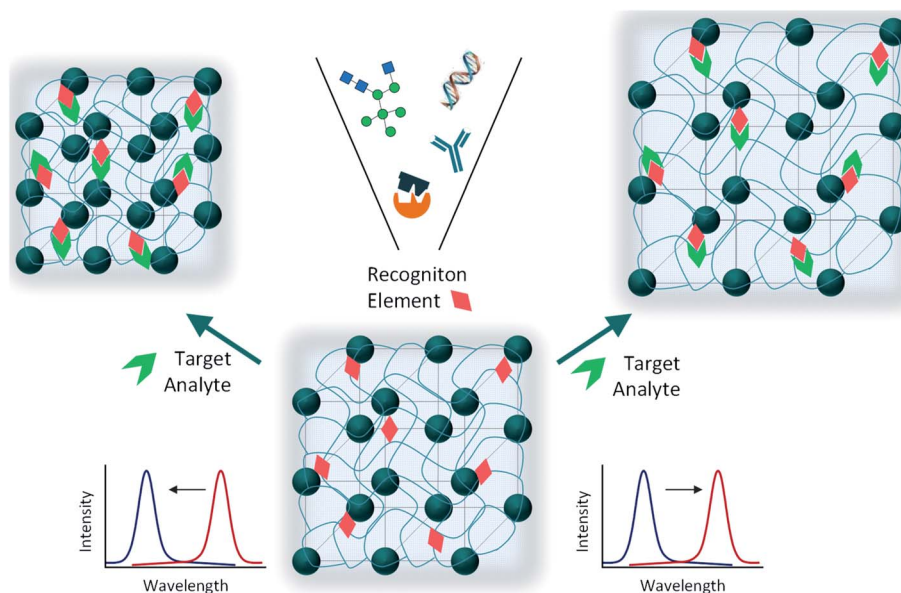
Fig. 16 Schematic illustration of a photonic hydrogel sensing material consisting of an embedded crystalline colloidal array surrounded by a polymer hydrogel network; the polymerized matrix contains molecular recognition elements (e.g., chemical moieties, aptamers, antibodies, enzymes) that, upon interaction with the target analyte, induce volume changes and, consequently, a shift in the observed reflectance.

hydrogel networks that have been successfully developed.[141,142] Additionally, multiplex smart polymers have been studied by introducing two or more sensing moieties. For example, Liu *et al.* (2015) built a pH and temperature dual responsive device, through spin-coating alternate layers of acrylic acid and *N*-iso-propylacrylamide copolymer and TiO_2 in order to obtain a multilayer 1D photonic stack (Fig. 17).[143]

However, the drawback of the aforementioned hydrogels is their low mechanical robustness, which limits their application for sensing mechanical stress, as the one generated by cells. Therefore, Yue *et al.* (2013) developed a photonic hydrogel that could not only respond to mechanical strain, but also to pH and temperature, through alternating layers of soft and hard polymers. The first layer was made of poly(acrylic acid) and poly(-acrylamide) (PAAm), whereas the second one consisted of poly(dodecylglyceryl itaconate) (PDGI). Whilst the increase of temperature and pH results in swelling of the soft layers of the hydrogel leading to a colour red shift, the mechanical compression shrinks the thickness of the gel and exhibits a blue shift.[144] By analysing the reflectance spectra, it was also possible to demonstrate the combined thermo-, pH-, and mechanochromatic behaviours.[144] Even if the hydrogel is multi-responsive, it is very difficult to distinguish which stimulus caused the observed changes on the sensor. Yue *et al.* (2016) solved this problem by creating two regions within a 1D photonic hydrogel composed of PDGI/PAAm. The native hydrogel is stress-sensitive, but does not respond to pH. By partially hydrolyzing PAAm into its acid form only in a certain region of the gel, the authors demonstrated that this specific region gained dual responsiveness, to pH and to mechanical stress (Fig. 18).[145]

More recently, microenvironment sensing and imaging has gained importance for detecting changes in microreactors and biological tissues. The photonic hydrogels so far discussed are unsuitable due to their bulk size. Therefore, Luo *et al.* (2020) developed chains of responsive hydrogel shells wrapping single 1D periodical structures of magnetic particles, which have a reduced size (tens of nanometers thick) and a fast response to

pH.[146] Interestingly, by using hydrogels with different functional groups it is also possible to extend the responsiveness of the nanochains to solvent and temperature, demonstrating them to be a versatile system.[146]

Generally, sensor platforms for biosensing need functionalization for target-specific recognition. Aptamers are short single-stranded oligonucleotides or small combinatorial proteins developed for selective recognition of target molecules. Besides specificity, aptamers also have good reproducibility and can be easily modified.[147] The toxic effects of heavy metal ions such as Hg^{2+} and Pb^{2+} are of concern, and efforts to improve their easy and accurate detection have been developed. Specific aptamer sequences were incorporated into a colloidal photonic crystal hydrogel network. Upon exposure to solutions of heavy metals, the aptamers change conformation by interacting with the target ions, leading to a shrinkage of the hydrogel and consequently, the quantitative detection is performed by analysing the blue shift in the Bragg diffraction peak.[147]

A similar principle relying on changes in the lattice spacing has been used to detect nerve agents, such as organophosphorus compounds (OPs). Different hydrogels were functionalized with enzymes, like organophosphorus hydrolase,[15] butyrylcholinesterase[148] or acetylcholinesterase.[149] In the study with organophosphorus hydrolase, the hydrolysis of the OP produces protons that create a pH gradient. As the hydrogel was also modified with phenolates, their protonation due to a lower pH inside the hydrogel exhibits a shrinkage and blue shifts the diffraction.[15] Interestingly, in the case of butyrylcholinesterase, the sarin agent binds irreversibly to the enzyme, creating an anionic phosphonyl species whose charge creates a Donnan potential and the hydrogel network swells causing a red shift.[148]

6. Molecularly imprinted photonic polymers

Molecularly Imprinted Polymers (MIPs) are created through the mixing of monomers, cross-linkers and the template molecule.
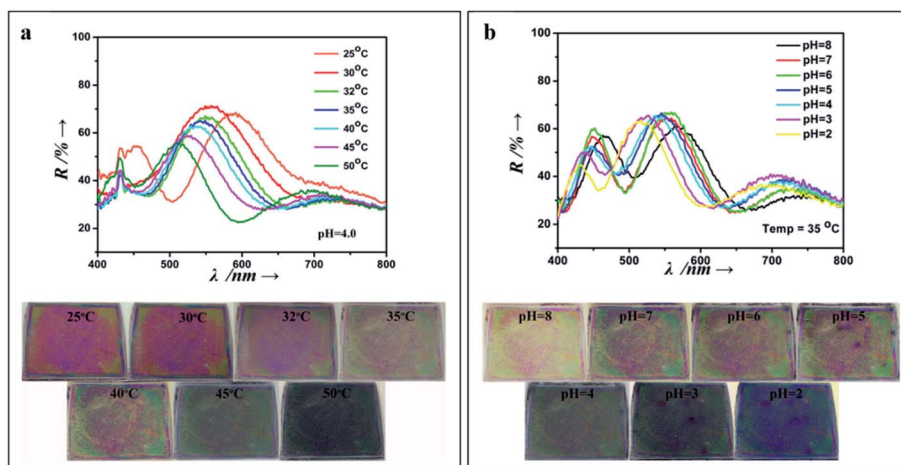

Fig. 17 1D photonic crystal hydrogel dually responsive to temperature and pH; reflectance spectra and photographs when exposed to (a) a range of temperatures (25 °C to 50 °C, at pH 4), and (b) a pH range (8 to 2, at a temperature of 35 °C) (reproduced with permission.[143] Copyright 2015, Elsevier).
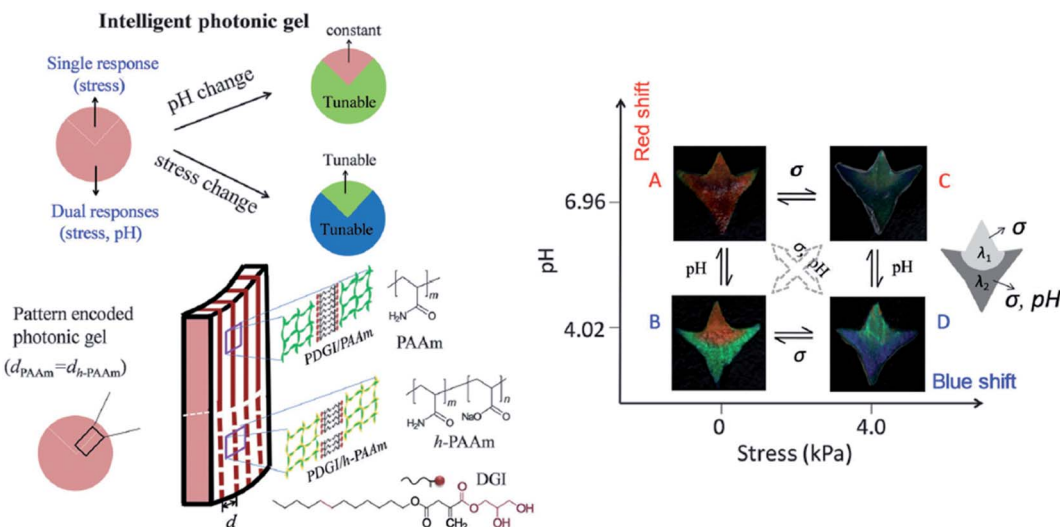
Fig. 18 Schematic illustration of a smart dual responsive photonic gel, able to respond to pH and compressive stress but distinguishing the source of the external stimuli by reversible colour changes in particular regions of the gel; the graph demonstrates that the upper region of the gel responds only to stress and the bottom to both pH and stress, presenting different colours (reproduced under the terms and conditions of the Creative Commons Attribution (CC-BY-NC) License.[145] Copyright 2016, The Royal Society of Chemistry).

After polymerization, the template is removed, leaving cavities with specific binding sites. If a photonic crystal is also introduced in the polymeric matrix, the presence and concentration of the target molecule influences the average refractive index and/or the swelling or shrinkage of the photonic polymer.[150] Therefore, photonic MIPs are seen as a winning strategy when it comes to developing highly specific and sensitive label-free sensors, and have been exploited to detect numerous target analytes.

The detection of amino acids and proteins is of great interest to the medical field since they may serve as disease indicators. Various research studies have developed inverse opal based photonic MIPs to detect chiral amino acids, namely L-proline,[151] and the glutamic acid derivative L-pyroglutamic acid.[152] These studies showed that the developed sensors responded to low concentrations and had chiral selectivity. Moreover, the recognition process could be visualized by the naked eye through a gradual colour change.[151,152] Photonic MIPs can also be modified with functional monomers, such as β-cyclodextrins that are cyclic oligosaccharides with a hydrophilic exterior and a hydrophobic cavity. The rationale of using β-cyclodextrins is related to an improved binding affinity of the hydrophobic cavity towards aromatic amino acids, as demonstrated by the photonic MIPs developed to detect L-phenylalanine[153] and L-tryptophan.[154] As for other macromolecules, imprinting proteins is more challenging than amino acids, due to their large size that hinders easy diffusion to the molecular cavities if they are buried in the polymer matrix.[155] To overcome this difficulty, strategies of surface imprinting have been pursued. The recognition of haemoglobin has been achieved by surface imprinting silica nanoparticles[156] and hollow silica spheres,[157] followed by suitable self-assembly into 3D photonic structures.

Other biomolecules can be sensed combining MIPs with photonic crystals. Most structures are obtained by self-assembly of colloidal nanoparticles, such as silica, PMMA or PS, followed by infiltration with the target template and pre-polymer mixture, polymerization and finally removal of the target template and colloidal nanoparticles (Fig. 19). The obtained highly ordered 3D porous films change their optical properties upon recognition of the analyte. Among the many different examples, such sensing systems have been used to detect glucose,[158] cholic acid,[159] cholesterol[160] and testosterone,[161] usually by the shift of Bragg diffraction.

Photonic MIPs as sensing materials have great potential to detect numerous other substances of pharmacological and toxicological concern in various media. This includes the monitoring of pesticides, drugs, food additives, and so on. For example, bisphenol A is an endocrine disruptor and a precursor of many plastics used in everyday life. Therefore, it is imperative to analyse its presence in our consumables. In fact, bisphenol A has been proven to bind the cavities of photonic MIP opals[162] (Fig. 20A) and inverse opals[163] thus, being easily detected. Also, creating a 2D planar defect layer, consisting of macropores of different sizes (Fig. 20B), within the molecularly imprinted photonic hydrogel was shown to be sensitive to bisphenol A, since the defect acts as an optical dopant and mechanical weakening agent.[164] Other sensors have been studied to analyse molecules of interest, like the food additive vanillin, obtaining a selective response and a shift on the Bragg diffraction peak.[165] Pharmacological molecules can also be detected using photonic MIPs, as is the case of the antibiotics tetracyclines[166,167] and chloramphenicol,[168,169] the nerve agent atropine[170] and the anaesthetic ketamine.[171] Finally, the herbicide atrazine,[172] the insecticide imidacloprid,[173] hydrolysates of organophosphorus compounds[174] and the flame retardants polybrominated diphenyl ethers[175] can also be detected using this type of sensor.
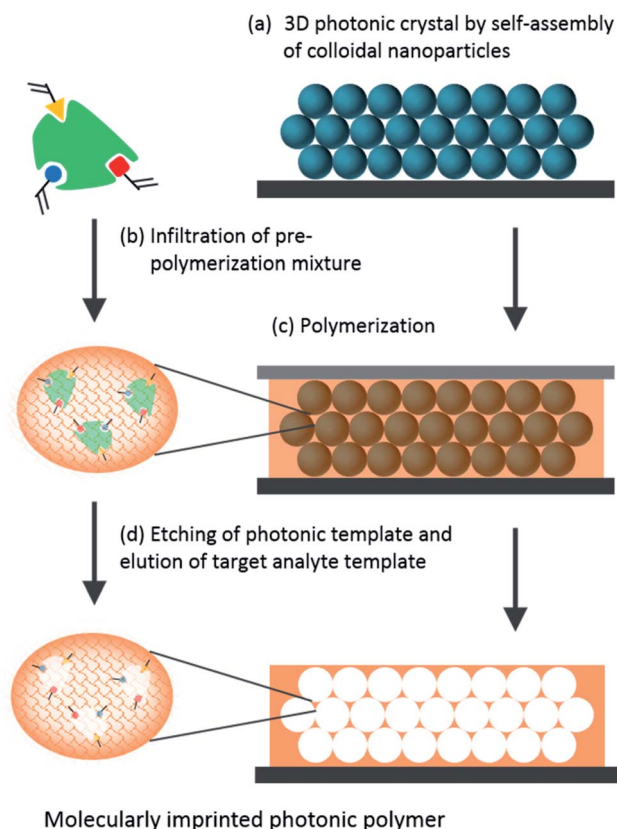
7. Photonics coupled with fluorescence

(a) 3D photonic crystal by self-assembly of colloidal nanoparticles

(b) Infiltration of pre-polymerization mixture

(c) Polymerization

(d) Etching of photonic template and elution of target analyte template

Molecularly imprinted photonic polymer

Fig. 19 Schematic illustration of the fabrication of an inverse opal photonic MIP film.

Multiplex assays have great importance in clinical diagnosis, drug screening and gene expression. Moreover, detection assays can be performed with suspension arrays instead of planar arrays, given their easy preparation, flexibility and greater diffusion. Colloidal crystal beads can be fabricated by a number of approaches and present stable, sharp reflection peaks and thus, may be used as encoded microcarriers in high-throughput assays.[132,176,177] Indeed, structural colouration as codes for carriers may be customized by varying the size of the nano-particles. Also, it is a clear advantage over the use of fluorescent dyes, since the colour is not quenched or bleached and does not interfere with the fluorescence signal from the labelling reporters.[178,179] Therefore, the combination of photonics and fluorescence brings great recognition benefits since the targets are identified by the photonic barcode beads and their abundance is quantified by the fluorescence intensity of the labels. Yan *et al.* (2017) used a suspension array of photonic agarose hydrogel microspheres that were used to immobilize single-stranded DNA (ssDNA) probes. The specific binding of the ssDNA probes to the metal ions Hg^{2+} and Ag^+ leads to a conformation change to double-stranded DNA hairpin structures where the SYBR Green I could intercalate, resulting in a strong fluorescent signal (Fig. 21).[179] Similar studies presented the use of photonic crystal microspheres as encoded beads to detect mycotoxins, such as aflatoxin B1, fumonisin B1 and ochratoxin A, using a multiplex chemiluminescence immuno-assay,[180] as well as to detect platelet-specific antibodies using
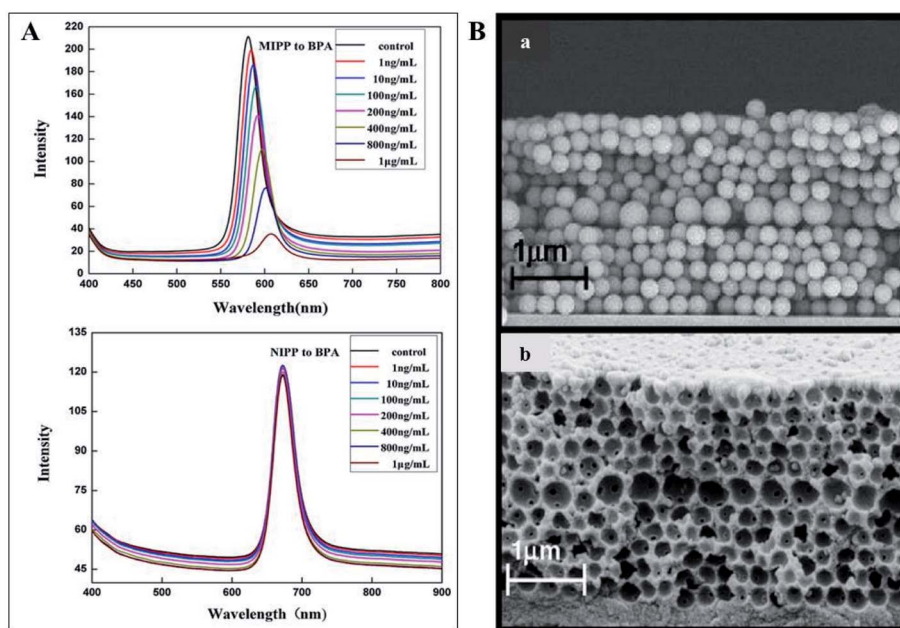
Fig. 20 (A) Optical responses of an opal photonic MIPP to several bisphenol A concentrations, showing an intensity decrease and a red shift, while the MIPP control showed no response (reproduced with permission.[162] Copyright 2012, Elsevier); (B) SEM image of a 2D photonic MIP structure to detect bisphenol A with an embedded planar defect layer on the opal (a) and inverse opal (b) assemblies (reproduced with permission.[164] Copyright 2011, Elsevier).
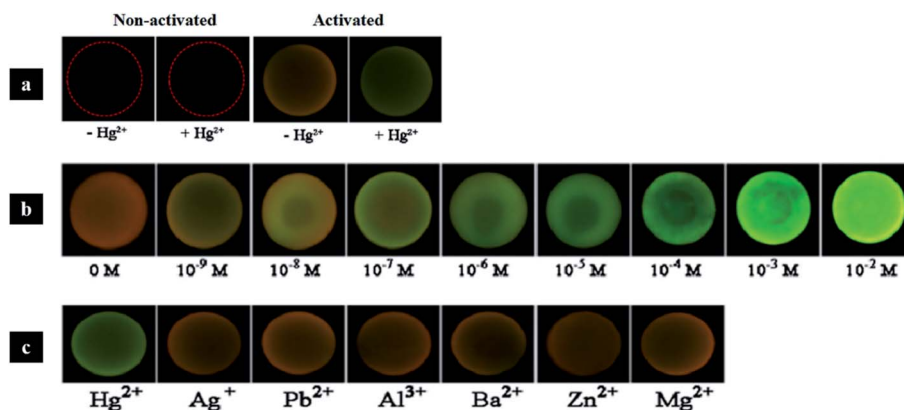
Fig. 21 Photonic crystal hydrogel microspheres for multiplex detection of metal ions: (a) control experiments without ssDNA probes (two of the left) and microspheres with ssDNA probes (two of the right); (b) in the presence of the probe, microspheres change colour to green, which is intensified with increasing concentrations of Hg^{2+}; (c) results of the selectivity tests with 1 μM of other metal ions, which were not detected (reproduced with permission.[179] Copyright 2017, Elsevier).

immunofluorescence.[181] Recently, a "flow-through" chip containing photonic crystal beads coated with capture antibodies has been designed for low-cost multiple detection of proteins, namely alpha-fetoprotein, IgG and the carcinoembryonic antigen based on sandwiched fluorescence immunoassays.[182]

Nevertheless, the number of codes that photonic crystals allows is limited, and the same applies to quantum dots (QDs). However, the combination of both gives rise to new codes. To this end, Li *et al.* (2014) successfully used QD-tagged photonic crystals to simultaneously detect the tumour markers alpha-fetoprotein and carcinoembryonic antigen, using the fluorescence of labelled antibodies as target signals.[183]

Another interesting application of photonic barcodes has been explored for microRNA quantification in a multiplex analysis.[184] In this study, photonic beads decorated with polydopamine were further modified with hairpin DNA probes and used for target-triggering cycle amplification and hybridization chain reaction (HCR) (Fig. 22). Once in the presence of the target microRNAs, these and helper DNAs were circularly employed to trigger the HCR, and the quantification was followed by fluorescence. The multiplex assays were demonstrated by observing a fluorescent signal only on the barcodes that had the specific binding between the probe and its target microRNA.[184]

8. Wearable photonic devices

Non-invasive devices for continuous, real-time monitoring of health parameters is an interesting line of research, which can be employed to measure heart rate, breathing and blood indicators, among others. Keeping track of these parameters is of great importance in military service, sports and firefighters' duties. For example, wearable photonic sensors can be included in contact lenses, wristbands or skin patches.[135]

Skin patches can be used to monitor several parameters. Gao *et al.* (2018) were inspired by the kirigami fish art to design a photonic sticker. The photonic crystals were assembled in the fish eyes (detection area) to enhance the fluorescence sensing of lactic acid and urea present in the sweat, while the sweat fluid

was directed from the tail through the stretchable channels to reach the sensors.[185] More recently, a wearable sensor based on inverse opal carbon rod electrodes introduced into the peacock tail, which can be attached to the eyelids, was successfully constructed to evaluate the concentration of glucose and
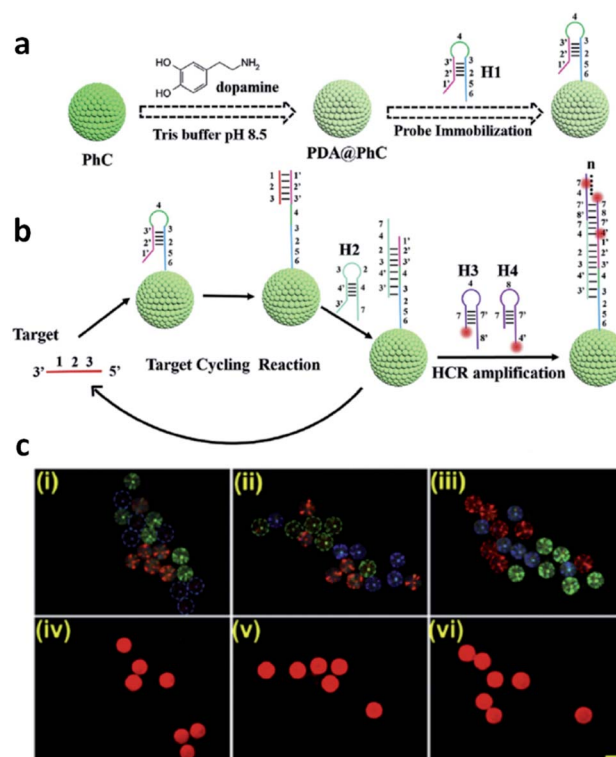
Fig. 22 Photonic barcodes for multiplex detection: (a) scheme illustrating the functionalization of the prepared barcodes with a probe; (b) scheme representing the microRNA detection based on target-triggering cycle amplification and hybridization chain reaction; (c) microscopy imaging, optical (i–iii) and fluorescent (iv–vi), of three types of photonic barcodes showing the selective detection of three different microRNAs, scale bar 200 μm (reproduced with permission.[184] Copyright 2019, Elsevier B. V.).

lactoferrin in tears, as well as the eye-movement frequency, which are related to diabetes.[186]

Another interesting application of wearable photonic colours was presented by Cullen *et al.* (2011). In this study, a photonic structure was created with multibeam interference lithography and using the SU-8 photoresist polymer. The structural colour changed or disappeared with blast exposure, due to the loss of the 3D structure. Therefore, the variation of colour allowed detecting the degree of shock-wave exposure, which in turn can be useful as an integrative device on soldiers' helmets in a war scenario to assess blast-induced traumatic brain injury.[187]

9. Drug delivery vehicles

Considering the described properties of photonic crystals, their applications are not entirely limited to sensors. Recent technical advances promote photonic-based systems to be more widely studied and developed in related biomedical areas, as in the case of drug delivery.

Drug delivery systems are used to safely transport therapeutic medicines to a certain part of the body, decreasing side effects and increasing chemical stability and therapeutic efficiency. Drug nanocarriers such as liposomes, dendrimers, micelles and nanospheres show great potential.[188] Particularly, the value of photonic systems in drug delivery has been recently explored. Zhang *et al.* (2015) used poly(*N*-isopropylacrylamide) hydrogel inverse opal particles, obtained from initial silica colloidal crystal beads, to monitor drug release in real-time. As a proof-of-concept, this study used fluorescein isothiocyanate (FITC)-dextran as a macromolecular model, and the reflection peak of the inverse opal blue shifted upon drug release. The uptake and discharge of the drugs were caused by the swelling and shrinking of the hydrogel, respectively, since it was designed to be temperature-responsive (Fig. 23).[189] These results showed that the macroporous structure provided channels for an active drug loading and release with simultaneous imaging of the process.

In a similar strategy, a thermoresponsive polymer was designed to trigger the synergistic release of macro and micro molecules, but in this case mesoporous silica nanoparticles were self-assembled in a droplet microfluidic device containing mesoporous colloidal photonic crystal particles with a large surface area and full of nanopores and interconnected nanochannels.[190] Song *et al.* (2017) also showed that a thin film of anodic aluminium oxide with nanopores in the shape of a honeycomb can be used for drug delivery. A layer-by-layer nanoassembly, where the model drug (gentamicin sulphate) was loaded, was introduced into the nanopores and also as stack layers. The system biocompatibility and the ability to optically report the release of the drug due to changes in the refractive index of the photonic structure demonstrate its potential as a drug delivery device.[191] Tao *et al.* (2018) developed 2D antimonene PEGylated nanosheets with photonic properties for drug loading applied to cancer therapeutics. This system responds to near-infrared light and acidic pH, showing a preference for tumour penetration and accumulation, as well as great imaging properties.[192] Similarly, Ji *et al.* (2018) produced an ultrathin photonic 2D boron nanosheet for drug delivery,
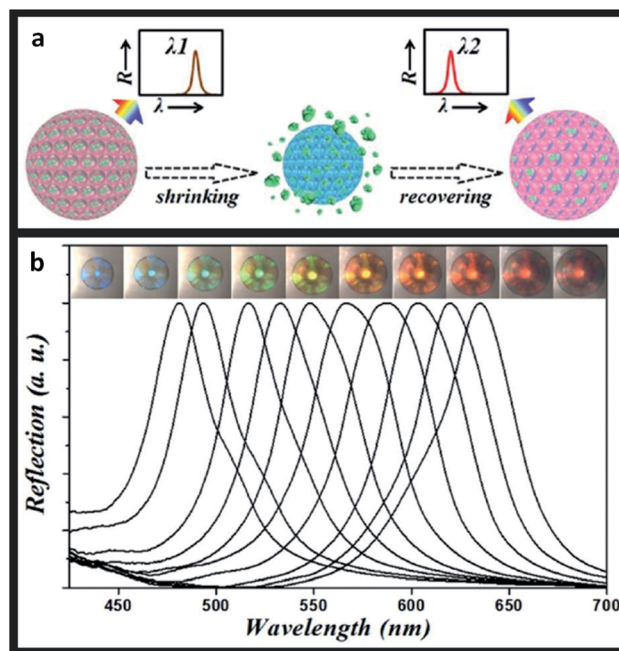

Fig. 23 Thermal-triggered drug release: (a) schematic illustration of the self-reporting thermoresponsive hydrogel inverse opal particles during drug release; (b) reflection images and spectra, where a temperature decrease leads to an increase in the volume of the particles (reproduced with permission.[189] Copyright 2015, The Royal Society of Chemistry).

which was responsive to pH and light for drug release, and with multiple features for promising applications in cancer therapy and imaging.[193]

10. Other bioinspired applications

The interaction of photonic beads with cells has also been pursued. In the context of metastatic cancer, barcodes have been functionalized with highly branched dendrimer-amplified aptamers to capture circulating tumour cells (CTCs).[194] Upon interaction with the cell affinity DNA aptamer probes, the cell adhesion on the barcode particles did not disturb the structural colour, which is quite useful in comparison to other encoding strategies. Also, the barcodes proved to be specific when multiple CTCs were targeted and enabled a subsequent efficient recovery of the cells.[194] This work is interesting as it pushes the boundaries of photonic barcodes to be used for cell culture, beyond the straightforward understanding of a sole sensor device. An analogous concept was pursued in the work of Fu *et al.* (2016) that presented a platform for drug screening based on cell spheroids-on-barcodes.[195] The barcode particles were encapsulated on hydrogel shells that allowed the development of an extracellular matrix for cell adhesion and growth. The advantage is related to the ability of distinguishing the biological response of each cell type encoded by specific diffraction peaks.[195] As a proof-of-concept, cytotoxicity tests were successfully performed on these barcode particles loaded with liver and tumour spheroids, demonstrating its feasibility as a new

platform for drug screening and expanding the prospect of organ-on-chips.

Other applications of hydrogels with structural colour have been demonstrated, namely through the possibility of presenting antibacterial and self-healing properties.[196] A hydrogel made of an inverse opal scaffold had integrated silver nanoparticles, whose constant release prevented bacterial adhesion and, consequently, hydrogel degradation and colour fading (Fig. 24). Moreover, such silver-tagged hydrogels filled with a high content of protein showed self-healing features while maintaining their vivid colours for a long time, even under conditions suitable for bacterial proliferation.[196] The applications are vast, from tissue engineering in a more biomedical view to further industrial perspectives.

The same applies to the recent use of structural colours in 3D-printing, resulting in colourful geometric pieces without the need of pigments. 3D objects made from photonic structures offer the capacity of having the desired colour, as well as acting as selective optical filters or light guides. A dendritic block copolymer made of benzyl and alkyl wedge-type monomers was already used to produce butterfly wings in the order of centimetres whose reflected colour could be tuned.[197] Another method to realize 3D-printed photonic crystals relies on using two-photon polymerization lithography that enables precise 3D pattern placement followed by using a heat-induced shrinking method. By using this technique, woodpile photonic crystal structures with fine-tuned lattice constants and a full range of colours were obtained (Fig. 25).[198]

Another expanding field is the use of photonic crystals in textiles in substitution of pigments, which enables high brightness and saturation with simultaneous resistance to colour fading due to light and washes.[199] Colloidal self-assembly of silica nanospheres was already proven to efficiently dye polyester fabrics with different colours according to the size of the particles.[200,201] The self-assembly occurs through filling the
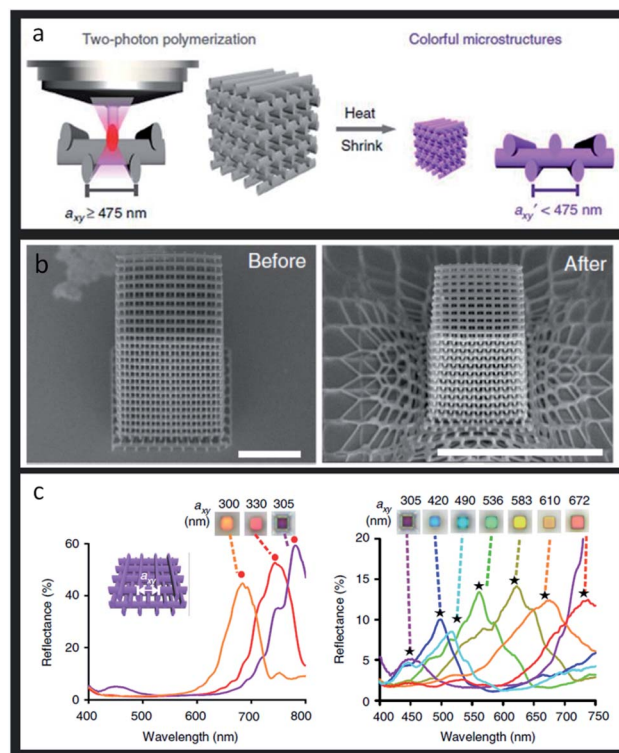

Fig. 25 Structural 3D colour printing: (a) scheme of woodpile photonic crystal obtained by two-photon polymerization; (b) SEM images (tilted-view) of a representative structure before and after heating, respectively, scale bars 10 μm; (c) reflectance spectra and reflection-mode micrographs of woodpiles where $a_{xy} = 300-350$ nm (left image) and $a_{xy} = 350-672$ nm (right image) (reproduced under the terms and conditions of the Creative Commons Attribution (CC-BY) License.[198] Copyright 2019, The Authors, published by Springer Nature).

gaps between the textile fibres, which is more successful in more hydrophobic fabrics.[201] Diverse structural colours, ranging from blue to red, can also be achieved using silica nanoparticles in cotton or silk fabrics.[202]

Many of the foreseen applications of structural colours have to consider the modulation of photonic crystal wettability. This is achieved at the fabrication stage by integrating surface topography (adjusting intrinsic and hierarchical roughness) and chemical composition (tuned by surface coating with hydrophilic/hydrophobic materials or by infiltrating liquids in the interstices of the structure).[203,204] There are typical examples in biological photonic structures where the wetting properties play a crucial role in the survival of organisms and bioinspire some interesting approaches to obtain liquid-repelling and anti-fouling surfaces with self-cleaning features.[204] For some applications, namely those that demand the use of photonic structures in wet environments, such as outdoor painting or as photonic coatings for solar heat reflection, it is critical to have an invariant PBG despite the weather. To this end, Kang *et al.* (2015) built a liquid-impermeable inverse opal inspired in nature, more particularly on springtails, which live in the soil. Their skin is made of a nanostructure of hexagonal voids and
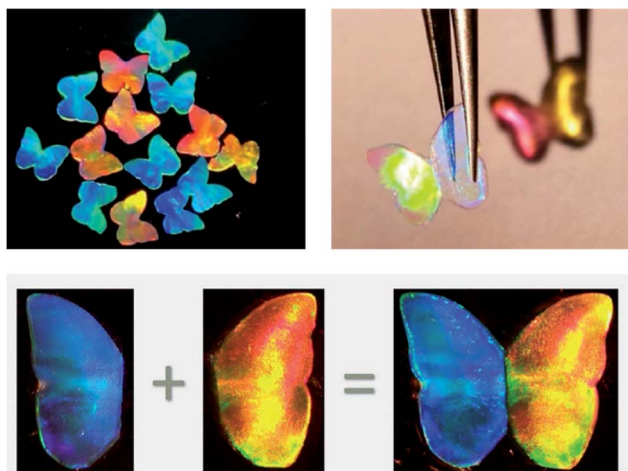

Fig. 24 Bioinspired antibacterial structural colour hydrogel tagged with silver nanoparticles, whose optical images demonstrate its integrity after self-healing (reproduced with permission.[196] Copyright 2017, American Chemical Society).
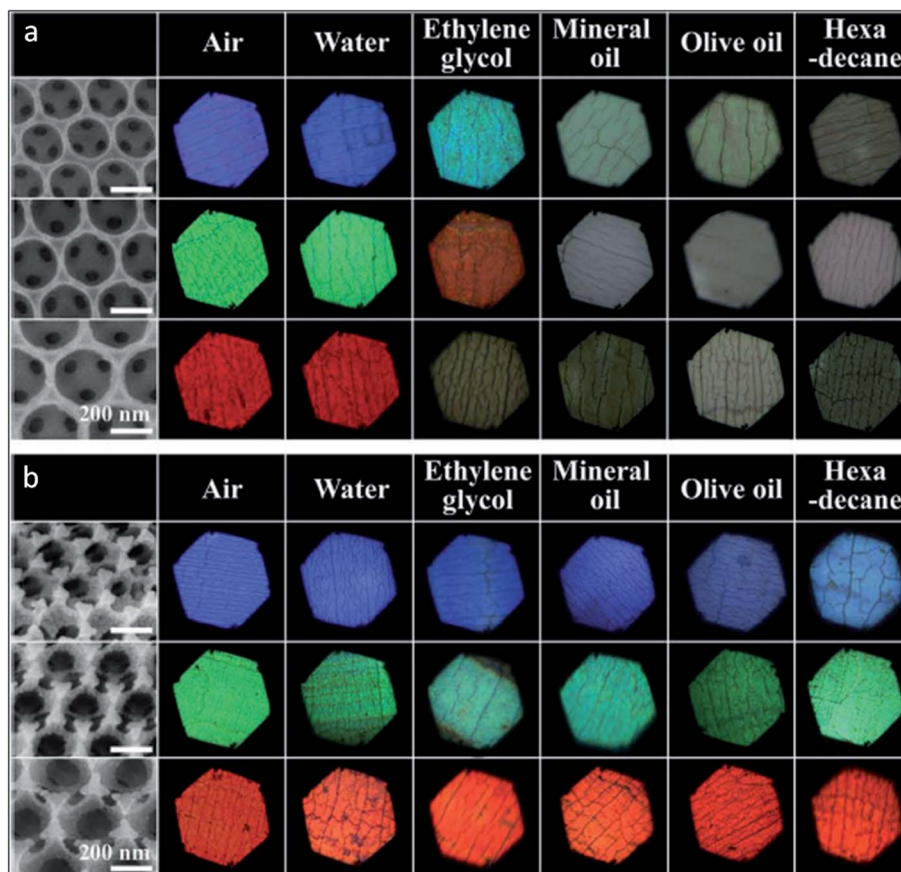
Fig. 26 Bioinspired liquid-impermeable inverse opal: SEM and optical microscope images of plain (a) and omniphobic (b) inverse opals, made of three sizes of silica nanoparticles (blue, green and red colours), and upon depositing five different liquids showing that the omniphobic nanoarchitecture retained its structural colour (reproduced with permission.[203] Copyright 2015, Wiley-VCH).

triangular posts with re-entrant geometry in the interstices having low surface energy. This allows pinning the air-liquid interface and confers omniphobic properties (Fig. 26).[203]

Interestingly, photonic crystals have also been studied for anti-counterfeiting purposes. Structural colour and patterns can be highly advantageous for authentication (e.g., watermarks) of
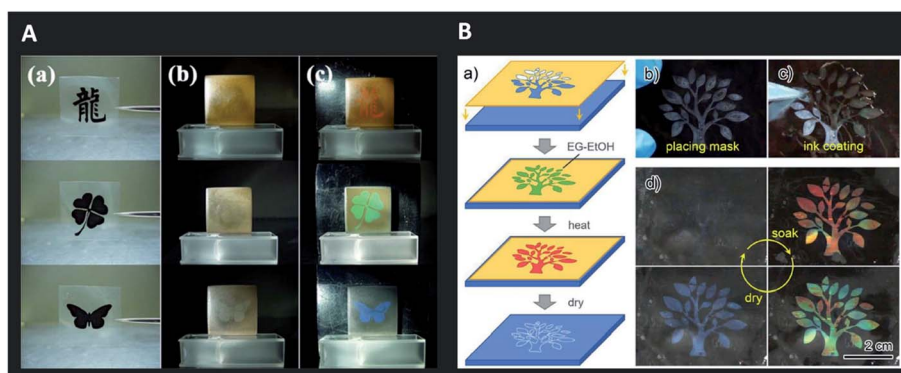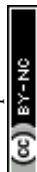

Fig. 27 Invisible photonic printing: (A) invisible print on a photonic paper (consisting of glycol droplets containing carbon-encapsulated super-paramagnetic colloidal nanoparticles and dispersed in a PDMS matrix) according to the designed masks used for UV-irradiation of the matrix (a); the pattern is invisible in the absence of a magnetic field (b) but visible when a magnetic field is applied (c) (only the unexposed or pattern region maintains the PDMS network intact and its magnetic-responsive photonic activities, leading to an ordered 1D structure and colour revealing) (reproduced under the terms and conditions of the Creative Commons Attribution (CC-BY-NC-ND) License.[212] Copyright 2013, Springer Nature); (B) schematic illustration of the procedure for printing the invisible photonic crystal patterns on a collapsed inverse opal macroporous polyurethane film (a), with respective images of mask placement (b) and ink coating (followed by thermal treatment and drying) (c); colour showing in the wet state upon soaking in ethanol–water (only the patterned "wet-heated" region recovers ordered macroporous structures and presents colour) and gradual disappearance with evaporation and returning to the dry state (d) (reproduced with permission.[215] Copyright 2019, American Chemical Society).

many daily life products. There are visible and invisible photonic prints for this purpose. Regarding the first class, the structural colour is altered due to external stimuli and it does not fade without the stimuli.[205] This way, it is possible to create small patterns like QR code designs, whose visibility depends on lighting conditions and coupled fluorescence.[206–211] Alternatively, invisible patterns are hidden until a stimulus is applied. Chemical swelling, mechanical stretching or magnetic fields, are some of the specific stimuli used for colour revealing (Fig. 27).[212–215] Designing such encrypted labels is challenging, because the information has to be strictly hidden until a specific trigger is given and should provide a fast and reversible response that has to be recognizable by the naked eye.

11. Conclusion and future perspectives

As a source of inspiration, some of the most amazing examples of photonic crystal patterns in natural systems have been introduced in this review. Having the ability to mimic the structural colours observed in nature, novel bioinspired materials and devices have been researched that have now blossomed into a myriad of applications. Photonic crystals owe their colour to the nanostructure of the material and, for that reason, have been considered an alternative to conventional pigments and dyes as a more sustainable approach to integrate and use colour.

The field of optical sensing has benefited the most from biomimicry and the ability to incorporate structural colour into the devices. In this review, the focus was mainly on biomedical sensors due to the great expectations for new, simpler, inexpensive and ameliorated optical methods for real-time detection of several chemicals and biomolecules. Label-free detection has been intensively developed in the areas of clinical diagnosis, food control and environmental monitoring, because of its clear advantages, with less time-consuming responses, high specificity and selectivity, as well as being a less expensive choice. As reviewed, the combination of structural colouration with (bio)polymers has revolutionized the area, attending to the numerous target analytes that have been successfully traced. Indeed, the ability to engineer polymer networks to respond to various stimuli and to modulate their interaction with biological systems, not only for diagnostic, but also for therapeutic purposes, has experienced huge progress.

Advanced biophotonic techniques are expected to have a growing relevance in medical diagnosis and treatment. Biologically derived and synthetic polymers comply with the necessary requirements of biocompatibility, biodegradability and biomechanics. To a lesser or greater extent, these materials also provide a high degree of modification due to their rich chemistry and can be fabricated by numerous methods. Still, future advances in this area may focus on improving the functionalities of polymer materials for fine-tuning their photonic responses. In particular, a rapid dynamic response to multiple external stimuli may constitute a benchmark that differentiates any photonic application to be translated into commercialization. To this end, one needs to master the design of materials with desired optical, biochemical and mechanical properties.

Although many aspects of photonic polymer fabrication have not been deeply addressed in the current review, there are many challenges, namely to acquire, in the same fabrication route, the ability to obtain upgraded crystalline structures using cost-effective techniques. Most of the photonic applications addressed rely on structures obtained by inexpensive self-assembly methods. Nonetheless, considering the increasing number of emerging fields where photonic materials may definitely have a promising contribution, it will be interesting in the future to observe a reinforcement in the likely synergy of fabrication techniques.

In conclusion, the perspective is that one can recreate nature's most dazzling colours and remarkable functions in order to design modern and sustainable solutions when it comes to biomedical sensors in point-of-care wearable devices, theragnostics, drug discovery, smart textiles, and related fields that are always searching for ground-breaking ideas to thrive.

Conflicts of interest

The authors declare no conflict of interest.

Acknowledgements

References

1 I. B. Burgess, M. Cončar and J. Aizenberg, *J. Mater. Chem. C*, 2013, **1**, 6075–6086.
2 J. Sun, B. Bhushan and J. Tong, *RSC Adv.*, 2013, **3**, 14862–14889.
3 Z. Wang and Z. Guo, *Chem. Commun.*, 2017, **53**, 12990–13011.
4 E. Armstrong and C. O'Dwyer, *J. Mater. Chem. C*, 2015, **3**, 6109–6143.
5 G. von Freymann, V. Kitaev, B. V. Lotsch and G. A. Ozin, *Chem. Soc. Rev.*, 2013, **42**, 2528–2554.
6 K. R. Phillips, G. T. England, S. Sunny, E. Shirman, T. Shirman, N. Vogel and J. Aizenberg, *Chem. Soc. Rev.*, 2016, **45**, 281–322.
7 C. Paquet and E. Kumacheva, *Mater. Today*, 2008, **11**, 48–56.
8 Y. Y. Diao, X. Y. Liu, G. W. Toh, L. Shi and J. Zi, *Adv. Funct. Mater.*, 2013, **23**, 5373–5380.
9 W. Li, Y. Wang, M. Li, L. P. Garbarini and F. G. Omenetto, *Adv. Mater.*, 2019, **31**, 1901036.

10 P. G. Gezer, A. Hsiao, J. L. Kokini and G. L. Liu, *J. Mater. Sci.*, 2016, **51**, 3806–3816.

11 G. Huang, Y. Yin, Z. Pan, M. Chen, L. Zhang, Y. Liu, Y. Zhang and J. Gao, *Biomacromolecules*, 2014, **15**, 4396–4402.

12 C. Fenzl, T. Hirsch and O. S. Wolfbeis, *Angew. Chem., Int. Ed. Engl.*, 2014, **53**, 3318–3335.

13 A. C. Sharma, T. Jana, R. Kesavamoorthy, L. Shi, M. A. Virji, D. N. Finegold and S. A. Asher, *J. Am. Chem. Soc.*, 2004, **126**, 2971–2977.

14 M. K. Maurer, S. E. Gould and P. J. Scott, *Sens. Actuators, B*, 2008, **134**, 736–742.

15 J. P. Walker, K. W. Kimble and S. A. Asher, *Anal. Bioanal. Chem.*, 2007, **389**, 2115–2124.

16 S. Tadepalli, J. M. Slocik, M. K. Gupta, R. R. Naik and S. Singamaneni, *Chem. Rev.*, 2017, **117**, 12705–12763.

17 E. S. A. Goerlitzer, R. N. Klupp Taylor and N. Vogel, *Adv. Mater.*, 2018, **30**, 1706654.

18 Y. Zhao, Z. Xie, H. Gu, C. Zhu and Z. Gu, *Chem. Soc. Rev.*, 2012, **41**, 3297–3317.

19 S. Vignolini, P. J. Rudall, A. V. Rowland, A. Reed, E. Moyroud, R. B. Faden, J. J. Baumberg, B. J. Glover and U. Steiner, *Proc. Natl. Acad. Sci. U. S. A.*, 2012, **109**, 15712–15715.

20 S. Z. M. Diah, S. B. Karman and I. C. Gebeshuber, *J. Nanomater.*, 2014, **2014**, 1–15.

21 W. E. Vargas, E. Avendano, M. Hernandez-Jimenez, D. E. Azofeifa, E. Libby, A. Solis and C. Barboza-Aguilar, *Biomimetics*, 2018, **3**, 1–20.

22 K. Michielsen and D. G. Stavenga, *J. R. Soc., Interface*, 2008, **5**, 85–94.

23 F. Mika, J. Matějková-Plšková, S. Jiwajinda, P. Dechkrong and M. Shiojiri, *Materials*, 2012, **5**, 754–771.

24 J. Zi, X. Yu, Y. Li, X. Hu, C. Xu, X. Wang, X. Liu and R. Fu, *Proc. Natl. Acad. Sci. U. S. A.*, 2003, **100**, 12576–12578.

25 D. W. Lee, *Nature*, 1991, **349**, 260–262.

26 D. W. Lee, G. T. Taylor and A. K. Irvine, *Int. J. Plant Sci.*, 2000, **161**, 297–300.

27 J. P. Vigneron, M. Rassart, Z. Vertesy, K. Kertesz, M. Sarrazin, L. P. Biro, D. Ertz and V. Lousse, *Phys. Rev. E: Stat., Nonlinear, Soft Matter Phys.*, 2005, **71**, 011906.

28 G. Strout, S. D. Russell, D. P. Pulsifer, S. Erten, A. Lakhtakia and D. W. Lee, *Ann. Bot.*, 2013, **112**, 1141–1148.

29 C. M. Eliason and M. D. Shawkey, *J. R. Soc., Interface*, 2012, **9**, 2279–2289.

30 D. G. Stavenga, B. D. Wilts, H. L. Leertouwer and T. Hariyama, *Philos. Trans. R. Soc., B*, 2011, **366**, 709–723.

31 S. Kinoshita, S. Yoshioka and K. Kawagoe, *Proc. R. Soc. London, Ser. B*, 2002, **269**, 1417–1421.

32 B. K. Hsiung, R. H. Siddique, D. G. Stavenga, J. C. Otto, M. C. Allen, Y. Liu, Y. F. Lu, D. D. Deheyn, M. D. Shawkey and T. A. Blackledge, *Nat. Commun.*, 2017, **8**, 2278.

33 B. D. Wilts, J. Otto and D. G. Stavenga, *Nanoscale Adv.*, 2020, **2**, 1122.

34 B. D. Wilts, K. Michielsen, H. De Raedt and D. G. Stavenga, *Proc. Natl. Acad. Sci. U. S. A.*, 2014, **111**, 4363–4368.

35 J. M. Medina, J. A. Diaz and P. Vukusic, *Opt. Express*, 2015, **23**, 10198–10212.

36 J. P. Vigneron, J. F. Colomer, M. Rassart, A. L. Ingram and V. Lousse, *Phys. Rev. E: Stat., Nonlinear, Soft Matter Phys.*, 2006, **73**, 021914.

37 J. Teyssier, S. V. Saenko, D. van der Marel and M. C. Milinkovitch, *Nat. Commun.*, 2015, **6**, 6368.

38 T. M. Trzeciak and P. Vukusic, *Phys. Rev. E: Stat., Nonlinear, Soft Matter Phys.*, 2009, **80**, 061908.

39 J. Romann, J. C. Valmalette, M. S. Chauton, G. Tranell, M. A. Einarsrud and O. Vadstein, *Sci. Rep.*, 2015, **5**, 17403.

40 M. Lopez-Garcia, N. Masters, H. E. O'Brien, J. Lennon, G. Atkinson, M. J. Cryan, R. Oulton and H. M. Whitney, *Sci. Adv.*, 2018, **4**, 1–8.

41 S. Yoshioka, B. Matsuhana, S. Tanaka, Y. Inouye, N. Oshima and S. Kinoshita, *J. R. Soc., Interface*, 2011, **8**, 56–66.

42 A. Yadav, A. Kaushik, Y. K. Mishra, V. Agrawal, A. Ahmadivand, K. Maliutina, Y. Liu, Z. Ouyang, W. Dong and G. J. Cheng, *Mater. Today Chem.*, 2020, **15**, 100208.

43 G. Rosolen and A. Cola, *2006 Conference on Optoelectronic and Microelectronic Materials and Devices*, 2006, pp. 66–69.

44 L. Wang, S. Zhang, Q. Wang, J. Chen, W. Jiang and R. T. Chen, *Appl. Phys. A*, 2009, **95**, 329–334.

45 M. Belotti, M. Galli, D. Bajoni, L. C. Andreani, G. Guizzetti, D. Decanini and Y. Chen, *Microelectron. Eng.*, 2004, **73–74**, 405–411.

46 G. Subramania and S. Y. Lin, *Appl. Phys. Lett.*, 2004, **85**, 5037–5039.

47 R. K. Bonam and J. G. Hartley, *J. Vac. Sci. Technol., B: Nanotechnol. Microelectron.: Mater., Process., Meas., Phenom.*, 2016, **34**, 1–6.

48 P. Ferrand, J. Seekamp, M. Egen, R. Zentel, S. G. Romanov and C. M. Sotomayor Torres, *Microelectron. Eng.*, 2004, **73–74**, 362–366.

49 Y. Chen, *Microelectron. Eng.*, 2015, **135**, 57–72.

50 L. Wu, Y. Xu and K. S. Wong, *Fabrication of Photonic Crystals Using Holographic Lithography*, Springer, 2015, pp. 213–239.

51 N. D. Lai, T. S. Zheng, D. B. Do, J. H. Lin and C. C. Hsu, *Appl. Phys. A*, 2010, **100**, 171–175.

52 S. Shaoxin, R. Xuechang, L. Shou, Y. Zhilin and Z. Yuanying, *Optical Engineering*, 2013, **52**, 095103.

53 S.-G. Park, T. Y. Jeon, H. C. Jeon, S.-M. Yang, J.-D. Kwon, C.-W. Mun, B. Cho, C. S. Kim and D.-H. Kim, *J. Mater. Chem. C*, 2014, **2**, 1957–1961.

54 L. L. Yuan and P. R. Herman, *Sci. Rep.*, 2016, **6**, 22294.

55 J. Li, Y. Liu, X. Xie, P. Zhang, B. Liang, L. Yan, J. Zhou, G. Kurizki, D. Jacobs, K. S. Wong and Y. Zhong, *Opt. Express*, 2008, **16**, 12899–12904.

56 J. Ma, K. S. Wong, S. Li, Z. Chen, J. Zhou and Y. Zhong, *J. Opt. Soc. Korea*, 2015, **19**, 63–68.

57 J. Lutkenhaus, D. Lowell, D. George, H. Zhang and Y. Lin, *Micromachines*, 2016, **7**, 1–11.

58 D. Lowell, J. Lutkenhaus, D. George, U. Philipose, B. Chen and Y. Lin, *Opt. Express*, 2017, **25**, 14444–14452.

59 S. Hassan, O. Sale, D. Lowell, N. Hurley and Y. Lin, *Photonics*, 2018, **5**, 34.

60 H. Schift, S. Park, B. Jung, C.-G. Choi, C.-S. Kee, S.-P. Han, K.-B. Yoon and J. Gobrecht, *Nanotechnology*, 2005, **16**, S261–S265.

61 M. Belotti, J. Torres, E. Roy, A. Pépin, Y. Chen, D. Gerace, L. C. Andreani and M. Galli, *J. Appl. Phys.*, 2006, **99**, 024309.

62 C. G. Choi, Y. T. Han and J. Kim, *SICE-ICASE International Joint Conference*, Busan, 2006, pp. 4893–4896.

63 S. H. Kim, K.-D. Lee, J.-Y. Kim, M.-K. Kwon and S.-J. Park, *Nanotechnology*, 2007, **18**, 055306.

64 T. Senn, J. Bischoff, N. Nüsse, M. Schoengen and B. Löchel, *Photonics Nanostructures: Fundam. Appl.*, 2011, **9**, 248–254.

65 J. J. Amsden, P. Domachuk, A. Gopinath, R. D. White, L. D. Negro, D. L. Kaplan and F. G. Omenetto, *Adv. Mater.*, 2010, **22**, 1746–1749.

66 A. Espinha, C. Dore, C. Matricardi, M. I. Alonso, A. R. Goni and A. Mihi, *Nat. Photonics*, 2018, **12**, 343–348.

67 G. Chu, A. Camposeo, R. Vilensky, G. Vasilyev, P. Martin, D. Pisignano and E. Zussman, *Matter*, 2019, **1**, 988–1000.

68 V. Bhingardive, L. Menahem and M. Schvartzman, *Nano Res.*, 2018, **11**, 2705–2714.

69 K. Feng, X. Gao, Z. Gu and Z. Jin, *ACS Sustainable Chem. Eng.*, 2019, **7**, 19062–19071.

70 D. Huang, M. Zeng, L. Wang, L. Zhang and Z. Cheng, *RSC Adv.*, 2018, **8**, 34839–34847.

71 J. M. Meijer, F. Hagemans, L. Rossi, D. V. Byelov, S. I. Castillo, A. Snigirev, I. Snigireva, A. P. Philipse and A. V. Petukhov, *Langmuir*, 2012, **28**, 7631–7638.

72 V. R. Dugyala and M. G. Basavaraj, *RSC Adv.*, 2015, **5**, 60079–60084.

73 J. L. Russell, G. H. Noel, J. M. Warren, N. L. Tran and T. E. Mallouk, *Langmuir*, 2017, **33**, 10366–10373.

74 J. Wang, X. Ma, L. Wei, G. Dai, X. Zhu, Y. Zhu, T. Mei, J. Li and X. Wang, *Mater. Express*, 2017, **7**, 351–360.

75 G. Liu, L. Zhou, Q. Fan, L. Chai and J. Shao, *J. Mater. Sci.*, 2015, **51**, 2859–2868.

76 L. Zhou, Y. Wu, L. Chai, G. Liu, Q. Fan and J. Shao, *Text. Res. J.*, 2016, **86**, 1973–1987.

77 H. Zhang and X. Liu, *Iran. Polym. J.*, 2017, **26**, 107–114.

78 S. Resende, M. F. Frasco and M. G. F. Sales, *Sens. Actuators, B*, 2020, **312**, 127947.

79 M. Ghosh, F. Fan and K. J. Stebe, *Langmuir*, 2007, **23**, 2180–2183.

80 C. Inui, Y. Tsuge, H. Kura, S. Fujihara, S. Shiratori and T. Sato, *Thin Solid Films*, 2008, **516**, 2454–2459.

81 C. Deleuze, B. Sarrat, F. Ehrenfeld, S. Perquis, C. Derail and L. Billon, *Phys. Chem. Chem. Phys.*, 2011, **13**, 10681–10689.

82 C. Hua, H. Xu, P. Zhang, X. Chen, Y. Lu, Y. Gan, J. Zhao and Y. Li, *Colloid Polym. Sci.*, 2017, **295**, 1655–1662.

83 W. Fan, M. Chen, S. Yang and L. Wu, *Sci. Rep.*, 2015, **5**, 12100.

84 D. T. Toolan, S. Fujii, S. J. Ebbens, Y. Nakamura and J. R. Howse, *Soft Matter*, 2014, **10**, 8804–8812.

85 A. B. D. Nandiyanto, T. Ogi, F. Iskandar and K. Okuyama, *Chem. Eng. J.*, 2011, **167**, 409–415.

86 Y. He, B. Zhu, X. Zeng, R. Yang, X. Lv and W. Yuan, *Thin Solid Films*, 2017, **639**, 98–106.

87 P. Jiang and M. J. McFarland, *J. Am. Chem. Soc.*, 2004, **126**, 13778–13786.

88 R. Pozas, A. Mihi, M. Ocaña and H. Míguez, *Adv. Mater.*, 2006, **18**, 1183–1187.

89 W. L. Min, P. Jiang and B. Jiang, *Nanotechnology*, 2008, **19**, 475604.

90 M. E. Pemble, M. Bardosova, I. M. Povey, R. H. Tredgold and D. Whitehead, *Phys. B*, 2007, **394**, 233–237.

91 M. Bardosova, M. E. Pemble, I. M. Povey and R. H. Tredgold, *Adv. Mater.*, 2010, **22**, 3104–3124.

92 G. Q. Liu, Z. S. Wang, Y. B. Liao, H. H. Hu and Y. Chen, *Appl. Opt.*, 2009, **48**, 2480–2484.

93 K. Wostyn, Y. Zhao, G. de Schaetzen, L. Hellemans, N. Matsuda, K. Clays and A. Persoons, *Langmuir*, 2003, **19**, 4465–4468.

94 T. Kohoutek, M. Parchine, M. Bardosova and M. E. Pemble, *Colloids Surf., A*, 2020, **593**, 124625.

95 L. Cui, Y. Zhang, J. Wang, Y. Ren, Y. Song and L. Jiang, *Macromol. Rapid Commun.*, 2009, **30**, 598–603.

96 Q. Zeng, C. Ding, Q. Li, W. Yuan, Y. Peng, J. Hu and K.-Q. Zhang, *RSC Adv.*, 2017, **7**, 8443–8452.

97 M. Ishii, T. Narita, Y. Hayata, A. Nishimura and K. Tachi, *Macromol. Mater. Eng.*, 2011, **296**, 687–692.

98 L. He, M. Wang, J. Ge and Y. Yin, *Acc. Chem. Res.*, 2012, **45**, 1431–1440.

99 M. Wang, L. He, W. Xu, X. Wang and Y. Yin, *Angew. Chem., Int. Ed. Engl.*, 2015, **54**, 7077–7081.

100 X. Xu, G. Friedman, K. D. Humfeld, S. A. Majetich and S. A. Asher, *Adv. Mater.*, 2001, **13**, 1681–1684.

101 X. Zhang, Y. Niu, J. Zhao and Y. Li, *New J. Chem.*, 2016, **40**, 9520–9525.

102 L. He, Y. Hu, H. Kim, J. Ge, S. Kwon and Y. Yin, *Nano Lett.*, 2010, **10**, 4708–4714.

103 H. Hu, Q.-W. Chen, K. Cheng and J. Tang, *J. Mater. Chem.*, 2012, **22**, 1021–1027.

104 J. Ge, J. Goebl, L. He, Z. Lu and Y. Yin, *Adv. Mater.*, 2009, **21**, 4259–4264.

105 R. Xuan and J. Ge, *J. Mater. Chem.*, 2012, **22**, 367–372.

106 Z. Li, M. Wang, X. Zhang, D. Wang, W. Xu and Y. Yin, *Nano Lett.*, 2019, **19**, 6673–6680.

107 A. Altube, Á. Blanco and C. López, *Mater. Lett.*, 2008, **62**, 2677–2680.

108 X. Liu, Y. Zhang, D. Ge, J. Zhao, Y. Li and F. Endres, *Phys. Chem. Chem. Phys.*, 2012, **14**, 5100–5105.

109 Z. Tan, Z.-H. Feng and L.-P. Yu, *J. Mater. Sci.: Mater. Electron.*, 2013, **24**, 2630–2635.

110 J.-P. Zhang and L.-P. Yu, *J. Mater. Sci.: Mater. Electron.*, 2014, **25**, 5646–5651.

111 E. Armstrong, M. O'Sullivan, J. O'Connell, J. D. Holmes and C. O'Dwyer, *J. Electrochem. Soc.*, 2015, **162**, D605–D612.

112 L. Pan, H. Xu, Y. Sun, J. Zhao and Y. Li, *Crystals*, 2016, **6**, 76.

113 J. L. Skinner, J. M. Andriolo, J. P. Murphy and B. M. Ross, *Nanophotonics*, 2016, **6**, 765–787.

114 D. Shan, E. Gerhard, C. Zhang, J. W. Tierney, D. Xie, Z. Liu and J. Yang, *Bioactive Materials*, 2018, **3**, 434–445.

115 M. Giese, L. K. Blusch, M. K. Khan, W. Y. Hamad and M. J. MacLachlan, *Angew. Chem., Int. Ed. Engl.*, 2014, **53**, 8880–8884.

116 B. Gao, H. Liu and Z. Gu, *Anal. Chem.*, 2016, **88**, 5424–5429.

117 M. Rolandi and R. Rolandi, *Adv. Colloid Interface Sci.*, 2014, **207**, 216–222.

118 T.-D. Nguyen, B. U. Peres, R. M. Carvalho and M. J. MacLachlan, *Adv. Funct. Mater.*, 2016, **26**, 2875–2881.

119 C. C. Ryan, J. A. M. Delezuk, A. Pavinatto, O. N. Oliveira, H. Fudouzi, M. E. Pemble and M. Bardosova, *J. Mater. Sci.*, 2016, **51**, 5388–5396.

120 C. Chen, Y. Liu, H. Wang, G. Chen, X. Wu, J. Ren, H. Zhang and Y. Zhao, *ACS Nano*, 2018, **12**, 10493–10500.

121 K. Min, S. Kim and S. Kim, *Proc. Natl. Acad. Sci. U. S. A.*, 2017, **114**, 6185–6190.

122 P. Tseng, S. Zhao, A. Golding, M. B. Applegate, A. N. Mitropoulos, D. L. Kaplan and F. G. Omenetto, *ACS Omega*, 2017, **2**, 470–477.

123 P. G. Gezer, S. Brodsky, A. Hsiao, G. L. Liu and J. L. Kokini, *Colloids Surf., B*, 2015, **135**, 433–440.

124 P. G. Gezer, G. L. Liu and J. L. Kokini, *Talanta*, 2016, **150**, 224–232.

125 M. E. Lynge, R. van der Westen, A. Postma and B. Stadler, *Nanoscale*, 2011, **3**, 4916–4928.

126 A. Kawamura, M. Kohri, G. Morimoto, Y. Nannichi, T. Taniguchi and K. Kishikawa, *Sci. Rep.*, 2016, **6**, 33984.

127 B. Yi and H. Shen, *J. Mater. Chem. C*, 2017, **5**, 8194–8200.

128 M. Kohri, K. Yanagimoto, A. Kawamura, K. Hamada, Y. Imai, T. Watanabe, T. Ono, T. Taniguchi and K. Kishikawa, *ACS Appl. Mater. Interfaces*, 2018, **10**, 7640–7648.

129 G. Chen, B. Yi, Y. Huang, Q. Liang and H. Shen, *Dyes Pigm.*, 2019, **161**, 464–469.

130 M. Kohri, K. Uradokoro, Y. Nannichi, A. Kawamura, T. Taniguchi and K. Kishikawa, *Photonics*, 2018, **5**, 36.

131 W. Zhu, H. Yang, Y. Lan, X. Yin, S. Wang, C. Wang, N. Gao and G. Li, *Adv. Mater. Interfaces*, 2016, **3**, 1600225.

132 P. Liu, T. Sheng, Z. Xie, J. Chen and Z. Gu, *ACS Appl. Mater. Interfaces*, 2018, **10**, 29378–29384.

133 S. Scarano, E. Pascale, P. Palladino, E. Fratini and M. Minunni, *Talanta*, 2018, **183**, 24–32.

134 H. Wang and K. Q. Zhang, *Sensors*, 2013, **13**, 4192–4213.

135 H. Inan, M. Poyraz, F. Inci, M. A. Lifson, M. Baday, B. T. Cunningham and U. Demirci, *Chem. Soc. Rev.*, 2017, **46**, 366–388.

136 L. Peponi, M. P. Arrieta, A. Mujica-Garcia and D. López, *Modification of Polymer Properties*, Elsevier, 2017, pp. 131–154.

137 A. K. Yetisen, H. Butt, L. R. Volpatti, I. Pavlichenko, M. Humar, S. J. Kwok, H. Koo, K. S. Kim, I. Naydenova, A. Khademhosseini, S. K. Hahn and S. H. Yun, *Biotechnol. Adv.*, 2016, **34**, 250–271.

138 S. A. Asher, V. L. Alexeev, A. V. Goponenko, A. C. Sharma, I. K. Lednev, C. S. Wilcox and D. N. Finegold, *J. Am. Chem. Soc.*, 2003, **125**, 3322–3329.

139 V. L. Alexeev, S. Das, D. N. Finegold and S. A. Asher, *Clin. Chem.*, 2004, **50**, 2353–2360.

140 Y.-J. Lee, S. A. Pruzinsky and P. V. Braun, *Langmuir*, 2004, **20**, 3096–3106.

141 X. Xu, A. V. Goponenko and S. A. Asher, *J. Am. Chem. Soc.*, 2008, **130**, 3113–3119.

142 H. Zhao, J. Gao, Z. Pan, G. Huang, X. Xu, Y. Song, R. Xue, W. Hong and H. Qiu, *J. Phys. Chem. C*, 2016, **120**, 11938–11946.

143 C. Liu, C. Yao, Y. Zhu, J. Ren and L. Ge, *Sens. Actuators, B*, 2015, **220**, 227–232.

144 Y. F. Yue, M. A. Haque, T. Kurokawa, T. Nakajima and J. P. Gong, *Adv. Mater.*, 2013, **25**, 3106–3110.

145 Y. Yue, X. Li, T. Kurokawa, M. Anamul Haque and J. P. Gong, *J. Mater. Chem. B*, 2016, **4**, 4104–4109.

146 W. Luo, Q. Cui, K. Fang, K. Chen, H. Ma and J. Guan, *Nano Lett.*, 2020, **20**, 803–811.

147 B. F. Ye, Y. J. Zhao, Y. Cheng, T. T. Li, Z. Y. Xie, X. W. Zhao and Z. Z. Gu, *Nanoscale*, 2012, **4**, 5998–6003.

148 J. Xu, C. Yan, C. Liu, C. Zhou, X. Hu and F. Qi, *IOP Conf. Ser.: Mater. Sci. Eng.*, 2017, **167**, 012024.

149 F. Qi, Y. Lan, Z. Meng, C. Yan, S. Li, M. Xue, Y. Wang, L. Qiu, X. He and X. Liu, *RSC Adv.*, 2018, **8**, 29385–29391.

150 W. Chen, Z. Meng, M. Xue and K. J. Shea, *Mol. Imprinting*, 2016, **4**, 1–12.

151 Y. Zhang, Z. Pan, Y. Yuan, Z. Sun, J. Ma, G. Huang, F. Xing and J. Gao, *Phys. Chem. Chem. Phys.*, 2013, **15**, 17250–17256.

152 Y.-X. Zhang, P.-Y. Zhao and L.-P. Yu, *Sens. Actuators, B*, 2013, **181**, 850–857.

153 X. Y. Liu, H. X. Fang and L. P. Yu, *Talanta*, 2013, **116**, 283–289.

154 Z. Yang, D. Shi, M. Chen and S. Liu, *Anal. Methods*, 2015, **7**, 8352–8359.

155 M. Dabrowski, P. Lach, M. Cieplak and W. Kutner, *Biosens. Bioelectron.*, 2018, **102**, 17–26.

156 W. Chen, W. Lei, M. Xue, F. Xue, Z.-h. Meng, W.-b. Zhang, F. Qu and K. J. Shea, *J. Mater. Chem. A*, 2014, **2**, 7165.

157 W. Chen, M. Xue, K. J. Shea, Z. Meng, Z. Yan, Z. Wang, F. Xue and F. Qu, *J. Biophotonics*, 2015, **8**, 838–845.

158 F. Xue, T.-r. Duan, S.-y. Huang, Q.-h. Wang, M. Xue and Z.-h. Meng, *J. Nanomater.*, 2013, **2013**, 1–6.

159 Z. Wu, X. Hu, C.-a. Tao, Y. Li, J. Liu, C. Yang, D. Shen and G. Li, *J. Mater. Chem.*, 2008, **18**, 5452–5458.

160 J. Li, Z. Zhang, S. Xu, L. Chen, N. Zhou, H. Xiong and H. Peng, *J. Mater. Chem.*, 2011, **21**, 19267.

161 A. J. Kadhem, S. Xiang, S. Nagel, C. H. Lin and M. Fidalgo de Cortalezzi, *Polymers*, 2018, **10**, 349.

162 C. Guo, C. Zhou, N. Sai, B. Ning, M. Liu, H. Chen and Z. Gao, *Sens. Actuators, B*, 2012, **166–167**, 17–23.

163 N. Griffete, H. Frederich, A. Maitre, S. Ravaine, M. M. Chehimi and C. Mangeney, *Langmuir*, 2012, **28**, 1005–1012.

164 N. Griffete, H. Frederich, A. Maitre, C. Schwob, S. Ravaine, B. Carbonnier, M. M. Chehimi and C. Mangeney, *J. Colloid Interface Sci.*, 2011, **364**, 18–23.

165 H. Peng, S. Wang, Z. Zhang, H. Xiong, J. Li, L. Chen and Y. Li, *J. Agric. Food Chem.*, 2012, **60**, 1921–1928.

166 L. Q. Wang, F. Y. Lin and L. P. Yu, *Analyst*, 2012, **137**, 3502–3509.

167 J. Hou, H. Zhang, Q. Yang, M. Li, L. Jiang and Y. Song, *Small*, 2015, **11**, 2738–2742.

168 C. Zhou, T. Wang, J. Liu, C. Guo, Y. Peng, J. Bai, M. Liu, J. Dong, N. Gao, B. Ning and Z. Gao, *Analyst*, 2012, **137**, 4469–4474.

169 N. Sai, Y. Wu, G. Yu, Z. Sun and G. Huang, *Talanta*, 2016, **161**, 1–7.

170 L. Meng, P. Meng, B. Tang, Q. Zhang and Y. Wang, *Forensic Sci. Int.*, 2013, **231**, 6–12.

171 L. Meng, P. Meng, Q. Zhang and Y. Wang, *Anal. Chim. Acta*, 2013, **771**, 86–94.

172 Z. Wu, C. A. Tao, C. Lin, D. Shen and G. Li, *Chemistry*, 2008, **14**, 11358–11368.

173 X. Wang, Z. Mu, R. Liu, Y. Pu and L. Yin, *Food Chem*, 2013, **141**, 3947–3953.

174 F. Liu, S. Huang, F. Xue, Y. Wang, Z. Meng and M. Xue, *Biosens Bioelectron*, 2012, **32**, 273–277.

175 D. Xu, W. Zhu, C. Wang, T. Tian, J. Li, Y. Lan, G. Zhang, D. Zhang and G. Li, *Chem Commun*, 2014, **50**, 14133–14136.

176 J. Hu, X.-W. Zhao, Y.-J. Zhao, J. Li, W.-Y. Xu, Z.-Y. Wen, M. Xu and Z.-Z. Gu, *J. Mater. Chem.*, 2009, **19**, 5730–5736.

177 Y. Zhao, Z. Xie, H. Gu, L. Jin, X. Zhao, B. Wang and Z. Gu, *NPG Asia Mater.*, 2012, **4**, e25.

178 X. Zhao, Y. Cao, F. Ito, H. H. Chen, K. Nagai, Y. H. Zhao and Z. Z. Gu, *Angew. Chem., Int. Ed. Engl.*, 2006, **45**, 6835–6838.

179 Z. Yan, C. Tian, X. Qu, W. Shen and B. Ye, *Colloids Surf., B*, 2017, **154**, 142–149.

180 K. Xu, Y. Sun, W. Li, J. Xu, B. Cao, Y. Jiang, T. Zheng, J. Li and D. Pan, *Analyst*, 2014, **139**, 771–777.

181 X. Kong, B. Ye, Z. Yang, B. Chen and Y. Ling, *Clin. Chim. Acta*, 2016, **458**, 72–77.

182 N. Chang, J. Zhai, B. Liu, J. Zhou, Z. Zeng and X. Zhao, *Lab Chip*, 2018, **18**, 3638–3644.

183 J. Li, H. Wang, S. Dong, P. Zhu, G. Diao and Z. Yang, *Chem. Commun.*, 2014, **50**, 14589–14592.

184 D. Zhang, F. Bian, L. Cai, T. Wang, T. Kong and Y. Zhao, *Biosens. Bioelectron.*, 2019, **143**, 111629.

185 B. Gao, A. Elbaz, Z. He, Z. Xie, H. Xu, S. Liu, E. Su, H. Liu and Z. Gu, *Advanced Materials Technologies*, 2018, **3**, 1700308.

186 B. Gao, Z. He, B. He and Z. Gu, *Sens. Actuators, B*, 2019, **288**, 734–741.

187 D. K. Cullen, K. D. Browne, Y. Xu, S. Adeeb, J. A. Wolf, R. M. McCarron, S. Yang, M. Chavko and D. H. Smith, *Journal of Neurotrauma*, 2011, **28**, 2307–2318.

188 C. Li, J. Wang, Y. Wang, H. Gao, G. Wei, Y. Huang, H. Yu, Y. Gan, Y. Wang, L. Mei, H. Chen, H. Hu, Z. Zhang and Y. Jin, *Acta Pharm. Sin. B*, 2019, **9**, 1145–1162.

189 B. Zhang, Y. Cheng, H. Wang, B. Ye, L. Shang, Y. Zhao and Z. Gu, *Nanoscale*, 2015, **7**, 10590–10594.

190 X. Gu, Y. Liu, G. Chen, H. Wang, C. Shao, Z. Chen, P. Lu and Y. Zhao, *ACS Appl. Mater. Interfaces*, 2018, **10**, 33936–33944.

191 C. Song, X. Che and L. Que, *Opt. Express*, 2017, **25**, 19391–19397.

192 W. Tao, X. Ji, X. Zhu, L. Li, J. Wang, Y. Zhang, P. E. Saw, W. Li, N. Kong, M. A. Islam, T. Gan, X. Zeng, H. Zhang, M. Mahmoudi, G. J. Tearney and O. C. Farokhzad, *Adv. Mater.*, 2018, **30**, 1802061.

193 X. Ji, N. Kong, J. Wang, W. Li, Y. Xiao, S. T. Gan, Y. Zhang, Y. Li, X. Song, Q. Xiong, S. Shi, Z. Li, W. Tao, H. Zhang, L. Mei and J. Shi, *Adv. Mater.*, 2018, 1803031.

194 F. Zheng, Y. Cheng, J. Wang, J. Lu, B. Zhang, Y. Zhao and Z. Gu, *Adv. Mater.*, 2014, **26**, 7333–7338.

195 F. Fu, L. Shang, F. Zheng, Z. Chen, H. Wang, J. Wang, Z. Gu and Y. Zhao, *ACS Appl. Mater. Interfaces*, 2016, **8**, 13840–13848.

196 Z. Chen, M. Mo, F. Fu, L. Shang, H. Wang, C. Liu and Y. Zhao, *ACS Appl. Mater. Interfaces*, 2017, **9**, 38901–38907.

197 B. M. Boyle, T. A. French, R. M. Pearson, B. G. McCarthy and G. M. Miyake, *ACS Nano*, 2017, **11**, 3052–3058.

198 Y. Liu, H. Wang, J. Ho, R. C. Ng, R. J. H. Ng, V. H. Hall-Chen, E. H. H. Koay, Z. Dong, H. Liu, C. W. Qiu, J. R. Greer and J. K. W. Yang, *Nat. Commun.*, 2019, **10**, 4340.

199 X. Gong, C. Hou, Q. Zhang, Y. Li and H. Wang, *J. Mater. Chem. C*, 2019, **7**, 4855–4862.

200 L. Zhou, Y. Wu, G. Liu, Y. Li, Q. Fan and J. Shao, *Coloration Technology*, 2015, **131**, 413–423.

201 Y. Li, L. Zhou, G. Zhang, G. Liu, Q. Fan and J. Shao, *Surf. Coat. Technol.*, 2017, **319**, 267–276.

202 W. Gao, M. Rigout and H. Owens, *J. Nanopart. Res.*, 2017, **19**, 303.

203 H. Kang, J. S. Lee, W. S. Chang and S. H. Kim, *Adv. Mater.*, 2015, **27**, 1282–1287.

204 N. Vogel, R. A. Belisle, B. Hatton, T. S. Wong and J. Aizenberg, *Nat. Commun.*, 2013, **4**(2167), 1–10.

205 M. Pan, L. Wang, S. Dou, J. Zhao, H. Xu, B. Wang, L. Zhang, X. Li, L. Pan and Y. Li, *Crystals*, 2019, **9**, 417.

206 J. Hou, H. Zhang, B. Su, M. Li, Q. Yang, L. Jiang and Y. Song, *Chem.–Asian J.*, 2016, **11**, 2680–2685.

207 Z. Meng, S. Wu, B. Tang, W. Ma and S. Zhang, *Nanoscale*, 2018, **10**, 14755–14762.

208 Y. Meng, F. Liu, M. Umair, B. Ju, S. Zhang and B. Tang, *Adv. Opt. Mater.*, 2018, **6**, 1701351.

209 H. S. Lee, T. S. Shim, H. Hwang, S.-M. Yang and S.-H. Kim, *Chem. Mater.*, 2013, **25**, 2684–2690.

210 H. Nam, K. Song, D. Ha and T. Kim, *Sci. Rep.*, 2016, **6**, 30885.

211 S. Shang, Q. Zhang, H. Wang and Y. Li, *J. Colloid Interface Sci.*, 2017, **485**, 18–24.

212 H. Hu, J. Tang, H. Zhong, Z. Xi, C. Chen and Q. Chen, *Sci. Rep.*, 2013, **3**, 1484.

213 T. Ding, G. Cao, C. G. Schafer, Q. Zhao, M. Gallei, S. K. Smoukov and J. J. Baumberg, *ACS Appl. Mater. Interfaces*, 2015, **7**, 13497–13502.

214 K. Zhong, J. Li, L. Liu, S. Van Cleuvenbergen, K. Song and K. Clays, *Adv. Mater.*, 2018, **30**, 1707246.

215 K. Chen, Y. Zhang and J. Ge, *ACS Appl. Mater. Interfaces*, 2019, **11**, 45256–45264.